PAIRING PLUS LONG RANGE FORCE FOR SINGLE CLOSED SHELL NUCLEI

BY

L. S. KISSLINGER AND R. A. SORENSEN

Synopsis

The low energy properties of nuclei are calculated, using a model which combines certain important features of the unified nuclear model and the independent-particle model with a two-body residual interaction. The residual interaction used has two parts, a pairing force and a long range part. Calculations are done for nuclei with a major closed proton or neutron shell, $A > 48$, for various values of the two strength parameters, using single-particle levels taken from experiment. In each region, the calculated energy levels and spins agree in considerable detail with systematic experimental data. In addition, the even-odd-A mass difference, the electromagnetic transition rates, and other properties are calculated and compared to experiment. The approximate $1/A$ dependence of the parameters is consistent with a volume force.

CONTENTS

I. Introduction

In the past several years, much evidence has been gathered by studying the low energy spectra of nuclei, and it has been possible to interpret many of the main observed features by the Unified Nuclear Model, i. e., in terms of the motions of individual particles in an effective nuclear potential[1] and collective excitations of rotational and vibrational character[2].

At the same time, attempts have been made to understand nuclear properties in terms of shell model particles interacting with a two-body force[3]. The detailed calculations in a single j shell for lighter nuclei have shown that in many cases it is possible to calculate approximately the energy levels by using specific nuclear forces. However, these calculations with pure configurations are not valid for heavier nuclei where configuration mixing becomes very important. Still, shell model calculations with a two-body force show that it is possible to derive many of the properties of nuclei with a few particles outside of closed shells by using a two-body force between particles which move in a well taken from experiment. However, for more than two or three particles in the system such calculations become extremely involved.

More recently, progress has been made in solving the many-body problem for specific models. Such work shows that it may be possible to derive the Unified Nuclear Model from a shell model description with the inclusion of a two-body interaction[4]. The first step was made by ELLIOTT who showed how the collective deformation and the associated rotational spectra can be obtained for particles in a harmonic oscillator potential interacting with a specific two-body force having angular dependence given by $P^{(2)}(\cos \theta)$, with θ representing the angle between the particles[5]. Later work[6] provided evidence that this is a general characteristic of the coupling scheme arising from interactions with a slow angular dependence, such as that of $P^{(2)}(\cos \theta)$. Since the low multipoles of the force are associated with the relatively long range part of the interaction, it therefore appears that this part of the nuclear interaction may be treated in terms of a deformed field acting

upon the individual nucleons, and is responsible for the associated collective nuclear properties.

The observed nuclear spectra clearly reveal, however, that there are important additional interaction effects which cannot be incorporated into the nuclear field. These residual interactions are responsible, for instance, for the shift of the intrinsic observed levels from the independent-particle prediction, for the collapse of the deformation with the approach to the closed shell regions, and for the energy gap observed in the intrinsic nuclear spectra. These two-body interactions should arise from the relatively short range part of the two-body interaction. A crucial problem has therefore been to develop methods to treat the effect of the short range part of the nuclear force in many-particle configurations.

A new approach to this problem was suggested by the recent development in the theory of superconductivity[7]. Methods have become available for treating the effects of a simplified interaction, the "pairing force", by which we mean a force which has constant matrix elements in a (jm), $(j-m)$ representation. I.e., the matrix elements of the pairing force between states of two particles in a j-level and two particles in a j'-level are proportional to $\sqrt{[(2j+1)/2][(2j'+1)/2]}$ if the total angular momentum in both states is zero, and vanishes otherwise. Such a force appears to represent many of the characteristic features of a short range interaction[8],[9]. It is hoped that specific differences between a short range force and the pairing force interaction can be calculated for individual properties when such differences are important.

The pairing force is a generalization of an interaction operator earlier introduced by RACAH, which characterizes the seniority coupling scheme for $(j)^n$ configurations. The new method therefore also leads to a generalization of the seniority concept in terms of the "quasi-particles". States of different seniority are separated by relatively large energies, and the gap in the nuclear excitation spectrum is thereby introduced, in analogy to that of the superconducting metals.

A nuclear model in which the interaction is represented by two simple components, the pairing force plus the long range part, usually represented by a quadrupole force, has been studied in some detail by BELYAEV[10] who showed that it contains the main qualitative features of the observed spectra. In particular, it accounts for the gradual transition from the closed shell regions to the regions of deformed nuclei with the associated vibrational and rotational modes of excitation.

Calculations with the model have so far, however, been based on a

greatly simplified single-particle level spectrum; especially the case of particles in a single degenerate level, such as a major shell in an oscillator field, have been treated[11]. A quantitative comparison with experimental data has therefore not been possible. To this purpose it is essential to introduce the proper succession and separation of the low lying single-particle levels available to the particles outside of closed shells.

In the present investigation we have attempted to perform such more realistic calculations, with a pairing force plus a $P^{(2)}$ force, based on available information about the single-particle level spectrum of the shell model, and to make a comparison with experimental data on the low energy nuclear properties.

For simplicity, we have restricted ourselves to nuclei in which either the neutrons or the protons are in a major closed shell. We shall refer to these as s.c.s. (single closed shell) nuclei. For this reason, we do not have to deal with the difficult problem of the short range interaction between neutrons and protons. These isotopes do not seem to possess a static equilibrium deformation and we can therefore use the spherical wave functions as a basis from which to start the calculation. The single-particle levels, when known, are taken from experiments on isotopes with one particle or hole outside of a double closed shell. In other cases, their positions are estimated from other experimental results and from theoretical calculations of the nuclear well.

Since the s.c.s. nuclei have a spherical equilibrium shape, the pairing force must in some sense be stronger than the $P^{(2)}$ force. For this reason, we first calculate the excitation energies of the s.c.s. nuclei with only the pairing force acting between shell model particles. We do this approximately, using the Bardeen solutions. Subsequently, the effect of the $P^{(2)}$ force is determined by the deformed field method. Of course, with such a simple force we cannot expect to derive the detailed quantitative properties of these nuclei, but rather attempt to find the main systematic features and to identify the main parts of the nuclear wave functions. We do expect that certain of the specific nuclear properties which are not given correctly by our wave functions might be derived from them by perturbation theory.

In Chapter II, the canonical transformation of the pairing Hamiltonian to the quasi-particle system is reviewed and the results are given which are important for the present calculation. We also describe the transformation to the collective coordinates to obtain the collective states. As an example of a possible interaction between quasi-particles, the perturbation theory results for the $P^{(2)}$ force are derived.

In Chapter III, the results for the energy levels of odd-A and even-A nuclei are presented for the various nuclear regions treated, along with discussions of the single-particle wells and the strength of the pairing and $P^{(2)}$ force in each case. In Chapter IV, the gap which results from our solutions is compared to that measured by the even-odd mass differences. In Chapter V, the expressions for the quadrupole moments are derived with our wave functions, and our theoretical predictions are compared to experiment. In Chapter VI, our calculated magnetic moments are compared to experiment and the additional shifts in the magnetic moments which are produced by a short range force differing from the pairing force are considered. In Chapter VII, the alterations of the electromagnetic transition rates caused by the pairing force and the $P^{(2)}$ force are investigated and the results compared to the experimental values.

II. The Hamiltonian and Approximate Solutions

A. The Hamiltonian

The basic assumption of this work is that, in the space of the wave functions for the low energy states of nuclei, the nuclear system can be represented as closed shells plus shell model particles which move in a well which changes only slowly as the number of particles changes, and which interact with a pairing force and a $P^{(2)}$ force.

Implicit in this assumption is the fact that the excitations of the core particles involve energies which are large compared to the excitations of the extra-core particles. To the extent that this is true we expect that the main effect of ignoring the core states as well as ignoring the states in the shells higher than the shell which we consider is to renormalize the parameters of the residual two-body interaction. Since we use a force which reproduces the low energy properties of s.c.s. nuclei, we implicitly include such contributions.

With regard to the long range part of the force, there are additional contributions from the core as are revealed by the polarization effects for one particle outside of a double closed shell, such as the enhanced $E2$ transitions in O^{17} and Pb^{207}. These are included in the present work by using a renormalized charge and quadrupole moment for the extra-core particles. The change in the positions of the single-particle levels with A is neglected within each s.c.s. region.

Letting $|0\rangle$, $|jm\rangle$, and $|j-m\rangle$ stand for the shell model particle

vacuum, and states with one shell model particle with angular momentum j- and z-component m and $-m$, respectively, the other quantum numbers being suppressed, we define the particle-creation operators

$$b^\dagger_{jm}|0\rangle = |jm\rangle$$
$$b^\dagger_{j-m}|0\rangle = |j-m\rangle = \tau|jm\rangle, \qquad\qquad \left.\begin{matrix} \\ \\ \end{matrix}\right\} (1)$$

where τ is the time-reversal operator*. In terms of these operators, the assumption is that the low energy states of s.c.s. nuclei are eigenstates of the Hamiltonian

$$H' = \sum_{jm} \varepsilon_j b^\dagger_{jm} b_{jm} - \frac{1}{2} G \sum_{jj'mm'} b^\dagger_{j'm'} b^\dagger_{j'-m'} b_{j-m} b_{jm}$$
$$- \frac{1}{2} \chi \sum_{\substack{j_1 j_2 j_1' j_2' \\ m_1 m_2 m_1' m_2'}} \langle j_1' m_1' j_2' m_2' | \mathfrak{P}^{(2)} | j_2 m_2 j_1 m_1 \rangle b^\dagger_{j_1' m_1'} b^\dagger_{j_2' m_2'} b_{j_2 m_2} b_{j_1 m_1}. \qquad (2)$$

In (2), ε_j are the single j shell particle levels, G is the strength parameter for the pairing force, and $\mathfrak{P}^{(2)}$ is the operator for the $P^{(2)}$ force (cf. II. C.), with a strength parameter χ.

Since the solution to the pairing part of the problem is simplified by transforming to a system in which the number of particles is not conserved, an auxiliary Hamiltonian is introduced which is related to H' by

$$H = H' - \lambda N = H' - \lambda \sum b^\dagger_{jm} b_{jm}, \qquad\qquad (3)$$

where λ, the chemical potential, is a Lagrangian multiplier included to take into account the constraint that for the solutions Ψ, $(\Psi|N|\Psi) = n$, the proper number of particles. Solutions to H with various values of G and χ are found for each s.c.s. region and a comparison shows that the A dependence of these parameters is consistent with their being a volume force.

* The states $|j-m\rangle$ have the phases $(-1)^{j-m} \times$ the states used by A. R. EDMONDS "Angular Momentum in Quantum Mechanics", Princeton University Press, Princeton, New Jersey (1957). Thus, the orbital spherical harmonics are defined as $i^l Y_{1m}$ and the spin states have an intrinsic phase of $\pi/2$ under time reversal. This choice of phases results in the same signs for the amplitudes of the $|jm\rangle|j-m\rangle$ states which are components of a $(j^2)_0$ state.

B. Pairing Force

1. *Canonical Transformation to an Independent-Particle Hamiltonian*

The ground state of the independent-particle Hamiltonian without residual interactions corresponds to filling of the single-particle levels with a sharp cutoff at the Fermi energy. I.e., all of the single-particle levels below the Fermi energy are definitely occupied and all of those above the Fermi energy are definitely unoccupied in the shell model ground state configurations. In the presence of the residual interactions, some of the particles are excited from the occupied single-particle levels to the levels which were unoccupied. The ground state of the Hamiltonian with a short range residual interaction corresponds to a diffuse distribution of the particles in the single-particle levels, with a region of energy near the Fermi energy, where the product, $U^2 V^2$, of the probability of occupation of a level, V^2, and the probability of non-occupation of a level, U^2, is not zero. Based on this physical picture, the method used in the present work is to express the ground state of the Hamiltonian with a pairing force residual interaction as an admixture of shell model configurations with the admixture coefficients determined by the U's and V's.

The energy level of an excited state of the independent-particle Hamiltonian without residual interactions is found simply by summing the single-particle energies of the excited configuration. In the presence of short range forces, the present method of solution allows one to identify once more independent modes of excitation, so that the energy level of an excited state eigenfunction with pairing forces present can be found approximately by simply adding the elementary excitation energies. Indeed, the independent excitations in the presence of the pairing forces are usually quite different from the single-particle shell model energy differences.

A convenient approximate solution for that part of Eq. (3) not including the $P^{(2)}$ force can be found by introducing the Bogolubov-Valatin canonical transformation into "quasi-particle" creation and annihilation operators[7]

$$
\left.
\begin{aligned}
\alpha_{jm} &= U_j b_{jm} - V_j b^{\dagger}_{j-m} \\
\beta_{jm} &= U_j b_{j-m} + V_j b^{\dagger}_{jm} \\
U_j^2 + V_j^2 &= 1.
\end{aligned}
\right\} \quad (4)
$$

Thus, a quasi-particle creation operator is a linear combination of a shell model particle and a shell model hole creation operator. The physical interpretation of U_j and V_j will be that V_j^2 is the probability of the pair

$(jm, j-m)$ being found in the ground state, while U_j^2, of course, is the prob-ability for non-occupancy, as can be seen from Eq. (8). Written in terms of these new Fermion operators, the Hamiltonian (in normal form) is

$$H^G = U + H_{11} + H_{20} + H_{int}, \tag{5}$$

where H^G refers to the Hamiltonian (3) without the $P^{(2)}$ force. U is independ-ent of quasi-particle operators, H_{11} is an operator of single quasi-particle type, i.e., each term has a factor $(\alpha^+\alpha + \beta^+\beta)$, and H_{20} creates or annihilates two quasi-particles. H_{int}, which contains products of four quasi-particle creation or annihilation operators, is ignored.[7), 10)] Therefore, when H_{20} is set identically equal to zero, the Hamiltonian (5) describes a system of non-interacting quasi-particles. The long range part of the two-body force will lead to an interaction between quasi-particles, as will be seen in the next section.

The result of setting $H_{20} = 0$ is the gap equation

$$\frac{G}{2} {\sum_j}' \frac{\Omega_j}{\sqrt{(\varepsilon_j - \lambda)^2 + \Delta^2}} = 1, \tag{6}$$

where

$$\left.\begin{array}{l} \Delta = G \sum_j \Omega_j U_j V_j \\[2mm] U_j^2 = \frac{1}{2}\left[1 + \frac{\varepsilon_j - \lambda}{\sqrt{(\varepsilon_j - \lambda)^2 + \Delta^2}}\right] \\[2mm] V_j^2 = \frac{1}{2}\left[1 - \frac{\varepsilon_j - \lambda}{\sqrt{(\varepsilon_j - \lambda)^2 + \Delta^2}}\right], \end{array}\right\} \tag{7}$$

and $\Omega_j = j + 1/2$ is the pair degeneracy of the j level. The essential problem in finding the solutions is determining λ and Δ, which are found by the simultaneous solution of the gap equation (6) together with the equation which results from fixing the mean number of particles (cf. (13)).

The wave functions are simply the quasi-particle creation operators operating on the quasi-particle vacuum. For an even-A nucleus, the ground state is the quasi-vacuum state, i.e., a state where all shell model particles are coupled in pairs to zero angular momentum. The excited states are the two, four, etc. quasi-particle states, corresponding to two, four, etc. element-ary excitations. In terms of the shell model particle states, the ground state of the even-A nuclei is

$$\Psi_0 = \Pi \underset{j}{\Pi} \underset{m>0}{\Pi} (U_j + V_j b^\dagger_{jm} b^\dagger_{j-m}) |0\rangle, \tag{8}$$

where $|0\rangle$ is the vacuum for a shell model particle, defined as $b|0\rangle = 0$. One obtains the one, two, etc. quasi-particle states by operating on Ψ_0 with quasi-particle creation operators.

2. Energy Spectrum

The ground state energy for even-A nuclei is

$$
\begin{aligned}
(\Psi_0 | H^G | \Psi_0) + \lambda n &= U + \lambda n \equiv U' \\
&= \sum_j{}' \Omega_j \varepsilon_j \left[1 - \frac{\varepsilon_j - \lambda}{\sqrt{(\varepsilon_j - \lambda)^2 + \Delta^2}} \right] - \sum_j{}' \frac{\Omega_j \Delta^2}{2\sqrt{(\varepsilon_j - \lambda)^2 + \Delta^2}} \\
&\quad - \frac{G}{4} \sum_j{}' \Omega_j \left[1 - \frac{\varepsilon_j - \lambda}{\sqrt{(\varepsilon_j - \lambda)^2 + \Delta^2}} \right]^2,
\end{aligned}
\tag{9}
$$

while the energy of a two quasi-particle state is

$$
\begin{aligned}
(\Psi(j_1 j_2) | H^G | \Psi(j_1 j_2)) + \lambda n &= U' + \sqrt{(\varepsilon_{j_1} - \lambda)^2 + \Delta^2} + \sqrt{(\varepsilon_{j_2} - \lambda)^2 + \Delta^2} \\
&= U' + E_{j_1} + E_{j_2},
\end{aligned}
\tag{10}
$$

where the two quasi-particles have angular momenta j_1 and j_2. From Eqs. (9) and (10) it is clear that there is a gap of at least 2Δ between the ground state and the two quasi-particle states of even nuclei. The ground state of odd-A nuclei is a one quasi-particle state, while the excited states are one, three, etc. quasi-particle states. Usually the three quasi-particle states are quite far removed in energy. Thus the energies of the ground and low excited states in odd-A nuclei are

$$(\Psi(j) | H^G | \Psi(j)) + \lambda n = U' + \sqrt{(\varepsilon_j - \lambda)^2 + \Delta^2} = U' + E_j, \tag{11}$$

where j is the angular momentum of the quasi-particle. Since there are several one quasi-particle states in each odd-A isotope, there is no gap like that in the even isotopes.

3. Number of Particles

For a state with r quasi-particles, $1, \ldots, r$, the expectation value of the number operator is

$$(\Psi_1 \ldots r \,|\, N \,|\, \Psi_1 \ldots r) = \sum_j{}' \Omega_j \left[1 - \frac{\varepsilon_j - \lambda}{\sqrt{(\varepsilon_j - \lambda)^2 + \Delta^2}} \right] + \sum_{i=1}^r{}' \frac{\varepsilon_i - \lambda}{\sqrt{(\varepsilon_i - \lambda)^2 + \Delta^2}}. \quad (12)$$

In even-A nuclei, the average number of particles in the ground state is

$$(\Psi_0 \,|\, N \,|\, \Psi_0) = n = \sum_j{}' \Omega_j \left[1 - \frac{\varepsilon_j - \lambda}{\sqrt{(\varepsilon_j - \lambda)^2 + \Delta^2}} \right]. \quad (13)$$

Given the shell model energies in a particular shell, (13) and (6) are sufficient to determine λ and Δ, for a given isotope, which in turn determine the ground state wave function and energy. The same values of λ and Δ are used for the excited states. This insures that those states are orthogonal to the ground states, and is expected to be a good approximation for states of few quasi-particles, which are the only ones considered in the present work. One could adjust λ and Δ for higher states. However, in this work, the average number of particles differs from the number N in the ground state. For instance, in a state with two quasi-particles of angular momentum k, the average number of particles differs from that of the ground state by

$$(\Psi(k, k) \,|\, N \,|\, \Psi(k, k)) - (\Psi_0 \,|\, N \,|\, \Psi_0) = 2 \frac{\varepsilon_k - \lambda}{\sqrt{(\varepsilon_k - \lambda)^2 + \Delta^2}}. \quad (14)$$

Although for the lowest quasi-particle states this quantity is small, since $\lambda \approx \varepsilon_k$ for the lowest elementary excitations, this variation in average number is sometimes nearly two for the distant two quasi-particle states. On the other hand, the error in the energy value of the state is not expected to be large since the solutions of H^G are stationary with respect to a variation in n. Still, a basic assumption of this work is that the excited states vary smoothly and slowly from isotope to isotope.

For the odd-A isotopes Eq. (13) is also used. In this case, the error in the average number of particles is small for the lowest states and unimportant in determining energy eigenvalues for the high one quasi-particle states for the same reason.

4. Accuracy of the Solutions

For a degenerate level, the Bardeen solutions give energies which are correct to order Ω^{-1} when compared to the exact solutions with the pairing force. In other words, the energies are good to order G/Δ, since $\Delta = G\Omega$ in this case. For a system of non-degenerate levels there is an effective pairing degeneracy,

$$\Omega_{\text{eff}} \equiv \frac{\Delta}{G} = \frac{1}{2} \sum_j{}' \frac{\Omega_j}{\sqrt{\left(\frac{\varepsilon_j - \lambda}{\Delta}\right)^2 + 1}}, \tag{15}$$

which indicates the accuracy. Therefore, even if the state near the Fermi surface has a low degeneracy, the solutions can give useful results so long as the pairing force scatters sufficiently to other states. One situation in which one might expect these solutions to be inaccurate is that in which a nuclear shell has a $j = 1/2$ subshell rather isolated from other levels. Such a situation may occur in the region of 50 neutrons. In this case, the solutions might be quite inaccurate for two or three isotopes near the point where the gap is small.

In addition to the small errors in the calculated energies which have been discussed above, the present approximation method introduces a characteristic uncertainty which arises directly from the fact that the wave functions are not eigenfunctions of the number of nuclear particles. This is the introduction of spurious states, and in particular of one spurious spin zero two quasi-particle state.[8], [9] Many levels are involved when the gap is large, so this spurious state is then distributed over many levels; there are, nevertheless, some situations in which one state is almost entirely spurious, as is the case in Pb^{206}. One can usually recognize such a situation when it occurs.

C. $P^{(2)}$ Force

1. Perturbation Theory

For the long range part of the shell model particle interaction we use the last term of (2) as two-body $P^{(2)}$ force:

$$
\begin{aligned}
H_{\text{long range}} &= -5/4\,\pi\,\frac{1}{2}\,\chi \sum_{ij}{}' F(r_i, r_j)\, P^{(2)}(\cos\theta_{ij}) \\
&= -\frac{1}{2}\chi \sum \langle j_1 m_1 j_2 m_2 \,|\, F(r_1, r_2) \sum_\mu (-1)^\mu Y_\mu^2(1)\, Y_{-\mu}^2(2) \,|\, j_2' m_2' j_1' m_1' \rangle \\
&\qquad b_{j_1 m_1}^\dagger b_{j_2 m_2}^\dagger b_{j_2' m_2'} b_{j_1' m_1'},
\end{aligned}
\tag{16}
$$

where $P^{(2)}(\cos\theta)$ is the Legendre polynomial of order two. The reason for this choice of force is that, for nuclei far from a closed shell, it can produce permanent quadrupole deformations which are experimentally observed; and for nuclei with or near closed shells, where its effect is weaker, it can provide an explanation for the observed quadrupole vibrational spectra.

Even for s.c.s. nuclei, which we consider, the long range interaction between the outside nucleons and the closed shell core plays an important role. However, we shall take the $P^{(2)}$ force acting only among the outside nucleons, and assume that the effect of the core can be included as a quadrupole force and charge renormalization for the outside particles.

For the perturbation treatment to follow, the radial dependence of the force is of less importance than the angular dependence given by $P^{(2)}$ (cos θ). In a j shell, for example, the energy spectrum is given entirely by the angular dependence of the force. For the evaluation of the matrix elements, we use the radial dependence $r_i^2 r_j^2$, as this is simply connected with the quadrupole field description of § II. C 2. This is the force, $r_i^2 r_j^2 P^{(2)}$ (cos θ), which is diagonal in the U (3) coupling scheme of Elliott.[5] For the evaluation of the radial matrix elements, harmonic oscillator wave functions are used.

If it is sufficiently weak, the $P^{(2)}$ force may be treated as a perturbation to the pairing force calculation. For this purpose, it is convenient to expand the force (16) in terms of creation and annihilation operators for quasi-particles:

$$H_{\text{long range}} = \frac{1}{2}\,\chi\,\{\mathfrak{P}_{00}{}^{(2)} + \mathfrak{P}_{20}{}^{(2)} + \mathfrak{P}_{11}{}^{(2)} + \mathfrak{P}_{40}{}^{(2)} + \mathfrak{P}_{31}{}^{(2)} + \mathfrak{P}_{22}{}^{(2)}\}, \qquad (17)$$

where, as in Belyaev, the subscripts refer to the number of creation and annihilation operators, respectively. The general form of the terms is given by Belyaev[10]. In first order perturbation theory, only $\mathfrak{P}_{11}{}^{(2)}$ and $\mathfrak{P}_{22}{}^{(2)}$ contribute to the relative level spacing. The effect of $\mathfrak{P}_{11}{}^{(2)}$ is to add to the energy of a quasi-particle of angular momentum j an amount

$$\langle \alpha_j | \mathfrak{P}_{11}{}^{(2)} | \alpha_j^\dagger \rangle = \chi \sum_{j_1}{}' \frac{5}{4\pi} \left(C_{0\,\frac{1}{2}\,\frac{1}{2}}^{2\,j\,j_1} \right)^2 \{U_j^2 - (U_{j_1}U_j - V_{j_1}V_j)^2\} \langle j\,|\,r^2\,|\,j_1 \rangle^2, \qquad (18)$$

where the "C"-symbol is a Clebsch-Gordan coefficient.

For the perturbation to have no effect on the number of particles in the ground state, to first order in the coupling constant χ, the chemical potential must be shifted simultaneously by an amount

$$\left.
\begin{aligned}
\Delta\lambda = \chi \sum_{jj_1}{}' \frac{5}{4\pi} \left(C_{0\,\frac{1}{2}\,\frac{1}{2}}^{2\,j\,j_1} \right)^2 \left(j + \frac{1}{2} \right) E_j^{-1} \left[(2\,U_j V_j)^2 V_{j_1}^2 - (2\,U_j V_j)(U_j^2 - V_j^2)\,U_{j_1}V_{j_1} \right] \\
\langle j\,|\,r^2\,|\,j_1 \rangle^2 \left[\sum_{j'} \left(j' + \frac{1}{2} \right) E_{j'}^{-1} (2\,U_{j'} V_{i'})^2 \right]^{-1}.
\end{aligned}
\right\} \qquad (19)$$

This causes an additional shift in energy for a quasi-particle of angular momentum j of an amount

$$\Delta E_j = -\Delta\lambda\,(U_j^2 - V_j^2). \tag{20}$$

If $G \ll \Delta$, the inclusion of this contribution is equivalent to the readjustment of the U's and V's so as to satisfy (6) and (13) with the inclusion of $P^{(2)}$ to first order in χ, thus leaving the quasi-particles independent except for the interaction part of the Hamiltonian, $\mathfrak{P}_{40}^{(2)} + \mathfrak{P}_{31}^{(2)} + \mathfrak{P}_{22}^{(2)}$. This contribution due to $\Delta\lambda$ is unimportant except for quasi-particles far from the Fermi surface.

The term $\mathfrak{P}_{22}^{(2)}$ has no effect on zero or one quasi-particle states, but for two quasi-particle states it splits the energy according to the total angular momentum, J, to which the two quasi-particles are coupled, thus breaking the degeneracy of the pairing Hamiltonian. For two quasi-particles of angular momentum j_1 and j_2 coupled to J, the energy shift is

$$
\begin{aligned}
&\frac{1}{2}\chi\big\langle[\alpha_{j_1}\beta_{j_2}]^J\,\mathfrak{P}_{22}^{(2)}\,[\beta_{j_2}^\dagger\alpha_{j_1}^\dagger]^J\big\rangle = -\frac{5}{4\pi}\frac{\chi}{2}\sqrt{(2j_1+1)(2j_2+1)} \\[6pt]
&\bigg\{(-1)^{j_1+j_2-J}\,C_{0\frac{1}{2}\frac{1}{2}}^{2j_1 j_1}\,C_{0\frac{1}{2}\frac{1}{2}}^{2j_2 j_2}\,W(j_1 j_2 j_1 j_2;\,J2)\langle j_1|r^2|j_1\rangle\langle j_2|r^2|j_2\rangle(U_1^2-V_1^2)(U_2^2-V_2^2) \\[6pt]
&\quad -(-1)^{j_1-j_2}\,C_{0\frac{1}{2}\frac{1}{2}}^{2j_1 j_2}\,C_{0\frac{1}{2}\frac{1}{2}}^{2j_2 j_1}\,W(j_1 j_2 j_2 j_1;\,J2)\langle j_1|r^2|j_2\rangle^2(U_1 U_2 - V_1 V_2)^2 \\[6pt]
&\quad +\frac{1}{5}(-1)^{j_1-j_2}\,C_{0\frac{1}{2}\frac{1}{2}}^{2j_1 j_2}\,C_{0\frac{1}{2}\frac{1}{2}}^{2j_2 j_1}\,\delta_{J2}\langle j_1|r^2|j_2\rangle^2(U_1 V_2 + U_2 V_1)^2\bigg\}.
\end{aligned}
\tag{21}
$$

where "W" is a Racah coefficient.

The first two terms on the right, which have the J dependence of the direct and exchange part of two shell model particles interacting with a $P^{(2)}$ force, arise from the normal interaction of the hole and particle part of the two quasi-particles with each other, the U, V factor expressing the fact that a hole and a particle interact with opposite sign from two particles or two holes. The third term, which only affects $J = 2$ states, arises from the mutual annihilation of the hole and particle parts of the quasi-particles and their subsequent creation through the $P^{(2)}$ force.

2. Collective Coordinates

It is easily seen from the experimental data on transition rates and excitation energies that this perturbation treatment of the long range force is not adequate for all states of most of the isotopes considered. First, the large

$B(E2)$ values for the deexcitation from the first excited 2^+ state of even nuclei to the 0^+ ground state make it impossible to explain this state as a two quasi-particle state perturbed by a $P^{(2)}$ force. The pairing correlations may introduce some enhancement of the $B(E2)$ values above a "single-particle" estimate, but in all cases they introduce less enhancement than that indicated by the collective treatment which follows. One finds, in the case of Pb^{206}, that the enhancement predicted by the collective treatment is 2.4 times that of the two quasi-particle 2^+ state with the largest enhancement. For Pb^{206}, where the effective charge (see Eq. (34)) is known from experiments in Pb^{207}, the transition rate agrees better with the collective $B(E2)$ than with the quasi-particle value. Thus, even though the collective approach may be least accurate in the Pb case, it may still be more accurate than the perturbation approach. In all other cases, the collective treatment increases the enhancement over that produced by pairing correlations alone by larger factors: a factor of about six for the Sn isotopes and about four for the Ni isotopes, for example. In these cases, the effective charge is not known from experiments analogous to those on Pb^{207}, but the collective treatment agrees with experimental transition rates for effective charges of about the magnitude of that in Pb^{207}, while larger effective charges would have to be used to obtain a fast enough decay from a perturbation treatment.

Second, the lowest 2^+ state is well below the two quasi-particle states produced by a pairing force of such strength as to be consistent with other data, this lowering also being the smallest in the case of the Pb isotopes. Since this 2^+ state must be constructed from the quasi-particle states, and is far separated from them in energy and of a different character from them, a non-perturbation treatment is necessary for this state.

We assume with Belyaev that we can define a collective parameter, Q, the quadrupole field or the total nuclear quadrupole moment, and that the main effect of the long range force can be described as an interaction of each particle with that field. Then,

$$H_{\text{long range}}(Q_\mu) = -\frac{1}{2}\chi\sum_\mu Q_\mu\hat{Q}_\mu, \tag{22}$$

where $\hat{Q}_\mu$, the quadrupole moment operator, is given by

$$\left.\begin{aligned}
\hat{Q} &= \sum_\nu q_{\nu\nu}^\mu\, 2\, V_\nu^2 + \sum_{\nu\nu'} q_{\nu\nu'}^\mu\,(U_\nu U_{\nu'} - V_\nu V_{\nu'})\,(\alpha_\nu^\dagger \alpha_{\nu'} + \beta_{\nu'}^\dagger \beta_\nu) \\
&\quad + \sum_{\nu\nu'} q_{\nu\nu'}^\mu\,(U_\nu V_{\nu'} + V_\nu U_{\nu'})\,(\alpha_\nu^\dagger \beta_{\nu'}^\dagger + \beta_\nu \alpha_{\nu'}),
\end{aligned}\right\} \tag{23}$$

and

$$q^{\mu}_{\nu\nu'} = \langle \nu \,|\, r^2 Y^2_{\mu} \,|\, \nu' \rangle \quad \text{with} \quad \nu \equiv jm. \tag{24}$$

Using harmonic oscillator wave functions, we have the selection rules that the parity of ν is the same as of ν' and

$$|j_{\nu} - j_{\nu'}| \leqslant 2. \tag{25}$$

We shall also require the condition of self-consistency: that the quadrupole moment of the outside nucleons associated with the Y^2_{μ} degree of freedom be equal to Q_{μ}. For this purpose we use a Lagrangian multiplier μ and the auxiliary Hamiltonian

$$H' = H - \mu \hat{Q} = H_{\text{pairing}} - \frac{1}{2} \chi Q \cdot \hat{Q} - \mu \hat{Q}, \tag{26}$$

where, for simplicity, we have dropped the subscript μ and consider for the moment only the contribution to the energy of the Y^2_0 quadrupole degree of freedom. To obtain the ground state energy of H we follow a method suggested by A. BOHR which is equivalent, within the approximations used, to that of Belyaev. If the quadrupole moment is not too large, the intrinsic ground state wave functions for (26) for even-A nuclei can be written in perturbation theory

$$\Psi(Q) = \Psi_0 - \left(\frac{1}{2} \chi Q + \mu \right) \sum_{\nu\nu'}' \frac{q_{\nu\nu'} (U_{\nu} V_{\nu'} + V_{\nu} U_{\nu'})}{E_{\nu} + E_{\nu'}} \alpha^{\dagger}_{\nu} \beta^{\dagger}_{\nu'} \Psi_0. \tag{27}$$

The Lagrangian multiplier μ is then fixed by the self-consistency condition

$$(\Psi(Q) \,|\, \hat{Q} \,|\, \Psi(Q)) = -2 \left(\frac{1}{2} \chi Q + \mu \right) \sum_{\nu\nu'}' \frac{q^2_{\nu\nu'} (U_{\nu} V_{\nu'} + V_{\nu} U_{\nu'})^2}{E_{\nu} + E_{\nu'}} = Q. \tag{28}$$

The ground state energy may then be calculated as a function of Q as

$$\left. \begin{aligned} (\Psi(Q) \,|\, H \,|\, \Psi(Q)) &= U' + \left\{ \left[4 \sum_{\nu\nu'}' \frac{q^2_{\nu\nu'} (U_{\nu} V_{\nu'} + V_{\nu} U_{\nu'})^2}{E_{\nu} + E_{\nu'}} \right]^{-1} - \frac{1}{2} \chi \right\} Q^2 \\ &= U' + \frac{1}{2} C Q^2, \end{aligned} \right\} \tag{29}$$

defining the restoring force parameter C. The rotationally invariant collective Hamiltonian, utilizing the five quadrupole degrees of freedom Q_{μ} associated with a Y^2_{μ} deformation, is then given by

$$H_{\text{coll}} = U' + \frac{1}{2} C \sum_{\mu} Q_{\mu}^2 + \frac{1}{2} B \sum_{\mu} \dot{Q}_{\mu}^2, \tag{30}$$

where the inertial parameter B is calculated in adiabatic perturbation theory to be[12)]

$$B = 2 \sum_{i}{}' \frac{(i \,|\, \delta/\delta Q \,|\, \Psi(Q))^2}{w_i - w_0} = \frac{1}{2} \sum{}' \frac{q_{\nu\nu'}^2 (U_\nu V_{\nu'} + V_\nu U_{\nu'})^2}{(E_\nu + E_{\nu'})^3} \left[\sum{}' \frac{q_{\nu\nu'}^2 (U_\nu V_{\nu'} + V_\nu U_{\nu'})^2}{E_\nu + E_{\nu'}} \right]^{-2}. \tag{31}$$

When quantized, the Hamiltonian (30) will lead to the spectrum associated with the harmonic qadrupole surface oscillations, the quanta being phonons of spin 2. With this description of the lowest 2^+ state, its properties can easily be obtained. The energy $0^+ - 2^+$ is given by

$$\hbar\omega = \sqrt{C/B}. \tag{32}$$

The ground state energy shift due to the $P^{(2)}$ force is obtained from the zero point energy

$$\Delta E_0 = \frac{5}{2} \hbar\omega(\chi) - \frac{5}{2} \hbar\omega(\chi = 0). \tag{33}$$

Assuming the 2^+ state to contain the entire quadrupole matrix element with the ground state, the $B(E2)$ value for excitation of the 2^+ from the 0^+ ground state is given by

$$B(E2) = \frac{5}{2} \frac{e_{\text{eff}}^2}{\sqrt{BC}}, \tag{34}$$

where e_{eff} is the effective charge of the extra-core nucleons. The effective charge of a nucleon is its own charge plus an additional positive charge arising from the fact that the extra-core nucleons can polarize the proton core to some extent. Experiments indicate that the effective charge of neutrons in Pb^{207} is about unity[13)]. In oxygen the proton core deformability seems to be somewhat less[14)]. For our calculations we take the effective charge of a neutron to be unity and of a proton to be two. The factor 5 occurs since the five quadrupole degrees of freedom contribute equally.

For the validity of this collective treatment of the $P^{(2)}$ force two conditions are required. First, the amplitude of the collective zero point oscillation, Q_{ave}, of the quadrupole moment Q must be large enough compared

to the fluctuations, δQ, of the quadrupole moment of the intrinsic state for the validity of Eq. (22). Second, the amplitude of collective oscillation must be small enough that the lowest order perturbation theory expression for (27) be sufficient. For the first condition it is required that

$$\left.\begin{aligned}\left(\frac{\delta Q}{Q_{ave}}\right)^2 &= \hbar\omega \sum' q_{\nu\nu'}^2 \frac{(U_\nu V_{\nu'} + V_\nu U_{\nu'})^2}{(E_\nu + E_{\nu'})^3} \cdot \sum' q_{\nu\nu'}^2 (U_\nu V_{\nu'} + V_\nu U_{\nu'})^2 \\ &\left[\sum' \frac{q_{\nu\nu'}^2 (U_\nu V_{\nu'} + V_\nu U_{\nu'})^2}{E_\nu + E_{\nu'}}\right]^{-2} < 1\,.\end{aligned}\right\} \quad (35)$$

This says roughly that the 2^+ level must lie well below the quasi-particle excitation energies, the same condition which is required for the adiabatic perturbation calculation of the inertial parameter B to be valid. In practice, this condition seems to be satisfied for the first 2^+ level in the s.c.s. nuclei considered, but in all cases the 0^+, 2^+, 4^+, second excited state lies near the top of or above the gap. Another way of stating condition (35) is that the collective state must collect a sufficient part of the total oscillator strength; i.e., that the collective $B(E2)$ be greater than the sum of the $B(E2)$'s for the various two quasi-particle 2^+ states. The second condition is a measure of the degree to which the collective oscillation is really harmonic. Although these conditions seem quite restrictive at first sight, in certain cases, at least, they are not. For one degenerate level of degeneracy 2Ω, the collective oscillation has been shown to be harmonic and correctly described by the above treatment[9] as long as the coupling parameter is not so large that one is too near the transition point at which a stable equilibrium deformation occurs. Thus, in this model, the only errors in the collective treatment are of order Ω^{-1} even though the 2^+ state lies just below or far below the quasi-particle excitations. In this work, the collective properties of s.c.s. even nuclei are described by the above method. This affects mainly the total binding energy and properties of the 2^+ first excited state. For the other states, this effect of the $P^{(2)}$ force on the excitation energies is estimated by first order perturbation theory, using the quasi-particle states given by the pairing force. This is not expected to describe correctly the splitting of the quasi-particle levels, since there may be other equally important effects from other components of the force which are not included in this calculation.

In the case of s.c.s. odd-A nuclei, one also expects that there should be collective electromagnetic transitions and that a perturbation treatment of the $P^{(2)}$ force is not adequate in all cases. Thus we use a collective treatment,

analogous to that above, for the effect of the $P^{(2)}$ force on the one quasi-particle levels of these nuclei, corresponding to the coupling of the quasi-particle to the collective oscillation. The intrinsic wave function in this case is

$$\Psi_\nu(Q) = \alpha_\nu^\dagger \Psi_0 - \left(\frac{1}{2}\chi Q + \mu\right) {\sum_{}}' \frac{q_{\nu'\nu''}(U_{\nu'}V_{\nu''} + V_{\nu'}U_{\nu''})}{E_{\nu'} + E_{\nu''}} \, \alpha_{\nu'}^\dagger \beta_{\nu''}^\dagger \alpha_\nu^\dagger \Psi_0. \quad (36)$$

The quadrupole moment is given by

$$\left.\begin{array}{l} (\Psi_\nu(Q) \,|\, \hat{Q} \,|\, \Psi_{\nu'}(Q)) \\[2mm] = q_{\nu\nu'}(U_\nu U_{\nu'} - V_\nu V_{\nu'}) - 2\left(\frac{1}{2}\chi Q + \mu\right) \underset{\underset{\nu'' \neq \nu}{\nu'''}}{{\sum}'} \frac{q_{\nu''\nu'''}^2 (U_{\nu''}V_{\nu'''} + V_{\nu''}U_{\nu'''})^2}{E_{\nu''} + E_{\nu'''}} \, \delta_{\nu\nu'} \end{array}\right\} \quad (37)$$

where the first term is the single-particle quadrupole moment of the quasi-particle. Ignoring the restriction on the ν'' sum, we may associate the second term with the collective quadrupole moment Q of the corresponding even system (cf. Eq. (28)). This approximation should be good to the extent that there are large numbers of states contributing to the sum. The Hamiltonian for the intrinsic state as a function of Q contains non-diagonal as well as diagonal terms in the one quasi-particle state and may be written

$$\left.\begin{array}{l} H = U' + \frac{1}{2}CQ^2 + \sum_\nu E_\nu(\alpha_\nu^\dagger \alpha_\nu + \beta_\nu^\dagger \beta_\nu) \\[3mm] + \chi \sum_{\nu\nu'} q_{\nu\nu'}(U_\nu U_{\nu'} - V_\nu V_{\nu'})(\alpha_\nu^\dagger \alpha_{\nu'} + \beta_{\nu'}^\dagger \beta_\nu) \, Q, \end{array}\right\} \quad (38)$$

the two terms in addition to those of (29) being the quasi-particle energy and the cross term from $1/2 \, \chi(Q + Q_{\mathrm{s.p.}})^2$. Assuming $Q \gg Q_{\mathrm{s.p.}}$, we have dropped the term quadratic in $Q_{\mathrm{s.p.}}$. In the collective Hamiltonian we utilize the five quadrupole degrees of freedom Q to produce the rotationally invariant expression

$$\left.\begin{array}{l} H_{\mathrm{coll}} = U' + \frac{1}{2}C\sum_\mu Q_\mu^2 + \frac{1}{2}B\sum_\mu \dot{Q}_\mu^2 + \sum_\nu E_\nu(\alpha_\nu^\dagger \alpha_\nu + \beta_\nu^\dagger \beta_\nu) \\[3mm] + \chi \sum_{\nu\nu'\mu} q_{\nu\nu'}^\mu (U_\nu U_{\nu'} - V_\nu V_{\nu'})(\alpha_\nu^\dagger \alpha_{\nu'} + \beta_{\nu'}^\dagger \beta_\nu) \, Q_\mu. \end{array}\right\} \quad (39)$$

C and B are given by (29) and (31), respectively. We thus ignore the difference in the inertial parameters for neighbouring even-even and odd-A nuclei (cf. Ref. 10, (136)).

This differs from the Bohr-Mottelson collective Hamiltonian for a vibrator coupled to a single particle by the factor $(U_\nu U_{\nu'} - V_\nu V_{\nu'})$ in H_{int}. The effect of this factor is that quasi-particles near the Fermi surface are more weakly coupled to the oscillation, while those farther from the Fermi surface are coupled more strongly. It also differs from the Bohr-Mottelson collective Hamiltonian in that the pairing energy is included. For simplicity, and because the coupling is not too strong for the single closed shell nuclei, we have calculated the effect of the last term in (39) by second order perturbation theory. In this case, the low lying one quasi-particle states receive an energy shift

$$\Delta E_j = -\frac{\chi^2}{2C}\sum_{j'} \frac{5}{4\pi}\left(C_{0\frac{1}{2}\frac{1}{2}}^{2jj'}\right)^2 \frac{\hbar\omega}{\hbar\omega + E_{j'}-E_j}(U_j U_{j'}-V_j V_{j'})^2 \langle j|r^2|j\rangle^2. \quad (40)$$

The Hamiltonian (39) will also have associated collective states, but there is not yet experimental evidence for these states for s.c.s. odd-A nuclei.

III. Energy Level Systematics

A. The Shell Model Particle Well

The energy levels of the s.c.s. nuclei, Eqs. (9), (10), and (11), are found by first calculating the quasi-particle energies, using a numerical solution of Eqs. (6) and (13). Next, the collective properties are determined as discussed in § II. C 2 and, finally, $P^{(2)}$ interactions between quasi-particles and their coupling to the vibrations are treated by the perturbation methods of § II. In order to proceed with such a calculation one must know the single-particle energies for a shell model particle moving in the effective well for one particle outside of a double closed shell, and must also know how these levels shift with A as one proceeds through the nuclear region.

When the levels of the one particle outside of the closed shell are not known, there is some uncertainty added to the calculation. There are some theoretical calculations for the level positions based on effective potentials with a few parameters, from which one has some knowledge of the well.[15],[16] Also, there are experimental energy level results from nuclei other than the s.c.s. nuclei treated in this work, which can be used to determine the single-particle energy levels in a particular region. If we wish to find, say, the single neutron levels for a region with a closed proton shell, we look at the energy levels of isotopes with one neutron and even numbers of protons outside

of the closed shells. For regions with large enough proton numbers, such that the neutrons and protons are filling different orbits ($Z \geq 28$), the short range interaction between the protons and neutrons is small (it is zero for our pairing force unless the particles are in the same levels). Therefore, it is reasonable to calculate the effect of the even numbers of protons on the odd neutron as a long range force for which an intermediate coupling phonon calculation can be used. Such calculations have had some qualitative success for heavy nuclei,[17] although it is not certain that such a simple treatment of the effect of the neutrons and the protons on each other is quantitatively correct. We have made only crude use of this method, with the hope of gaining some knowledge of the single-particle levels in a particular region, working backward from the known experimental levels to try to find the values of the single-particle levels which are consistent with the experimental data. In this work, both of these methods have been used to determine the single-particle levels. However, the lack of experimental data and single-particle levels is a major uncertainty in this work.

The rate and manner in which the single-particle states shift with A are difficult to establish. However, if the dependence is something like $A^{-1/3}$, then our results are very little affected by this motion in most regions. In none of our s.c.s. regions is there direct evidence that the change in the single-particle energies with A affects the accuracy of our calculations, particularly in view of the uncertainty in the level positions. Still, there is a possibility that, when the number of particles changes as much as it does in, say, the Sn region, there are systematic deviations introduced. The change in the single-particle levels with A does apparently play an important role in determining the levels of $N = 50$. In this work, we have not changed the energy level separation of the levels in any one region, although we have investigated the variation in the depth of the well in the binding energy calculation.

B. The Choice of Parameters]

Once the single-particle well with its energy levels has been established for a given closed shell region, the consequences of our model are determined in terms of the two coupling parameters G and χ. It is well established that a short range residual nuclear force is necessary in a description of nuclei. The strength of this force, which is simulated in our calculation by the pairing force with its coupling parameter G, can be determined in many ways. For example, the systematic experimental odd-even mass difference

discussed in the next section is affected very little by the long range force, and can thus be used to determine G to about $30^0/_0$ in most regions. Closely related to this is the so-called energy gap of even-even nuclei.[18] In heavy highly deformed nuclei, this shows up in the fact that the first intrinsic excited state of an even-even nucleus usually lies above 1 Mev, while very low intrinsic excitations often occur in the neighbouring odd-A nuclei. In the case of the spherically symmetric s.c.s. even-A nuclei which we consider, there is also an energy gap in which only the collective 2^+ level occurs. The position in energy of the two quasi-particle excited states, which lie at or above the top of the gap, depends strongly upon the strength of the coupling parameter G. In cases where an experimentally observed excited state can be uniquely associated with a two quasi-particle excitation, one can make an independent estimate of G. Such a situation occurs in the case of observed states of high spin, J, and odd parity. First, the two quasi-particles forming such a state must have opposite parity. In each mass region considered there is always just one single-particle state of parity opposite from the rest, and this must be the j-state of one of the quasi-particles. The high J value of the excited state can then determine rather uniquely which is the second quasi-particle. The 9^- levels in Pb^{204} and Pb^{202} and the 7^- level in Sn^{120} permit such a determination to be made. This leads to a value of G between $23/A$ and $30/A$ for Pb and about $19/A$ for Sn. The $P^{(2)}$ force is included as a perturbation in this determination.

Once the value of G has been determined, the coupling parameter χ of the long range part of the force may be determined from the quantities it most affects, namely the position of the first 2^+ states of the even-A nuclei and the $B(E2)$ value for the $(0^+ \rightarrow 2^+)$ transition. For any one isotope the experimental excitation energy can be fit with the theoretical value by an appropriate choice of χ, a larger G requiring a correspondingly larger χ. However, we require that in any one mass region (corresponding to a particular double closed shell with one kind of particles outside) one value of G and χ or rather X (cf. below, Eq. (41)) be used for all the isotopes. With this requirement, one can determine the G and χ which together give the best fit to the position of the first excited 2^+ level as a function of Z or N in an entire mass region. Where good comparison can be made, the G determined this way is in agreement with that determined by the previous methods.

Although the $B(E2)$ value depends strongly on χ, it also contains a factor e_{eff}^2 which may vary somewhat from shell to shell. Thus, except in the case of the Pb isotopes for which e_{eff} is independently determined

from $E2$ transition rates in Pb^{207}, one can determine e_{eff} only from the $B(E2)$ values and, assuming e_{eff} to be constant in one mass region, see whether the variation from isotope to isotope is consistent with experiment. The G and χ determined for Pb from the $B(E2)$ value of Pb^{206} are consistent with the values determined from the previous methods.

Although we did not try to determine uniquely the best values for G and χ, it is seen that both have a simple and smooth A dependence in going from region to region. G varies more or less as A^{-1}, the value $19A^{-1}$ Mev being better for the regions from $N = 28$ to Sn, and $G = 23A^{-1}$ being better for $N = 82$ and Pb. The corresponding value of χ in going from region to region varies more or less as $A^{-7/3}$ is expected (cf. Ref. 10, (93)). We consider instead the quantity X defined by

$$X = \chi \frac{5}{4\pi} \langle j \, | \, r^2 \, | \, j \rangle_u^2 = \chi \frac{5}{4\hbar} \left(\frac{\hbar}{M\omega_0} \right)^2 \left(n + \frac{3}{2} \right)^2, \tag{41}$$

where M is the nucleon mass, $\hbar\omega_0 = 41A^{-1/3}$ Mev, n is the total number of oscillator quanta associated with most of the single-particle (harmonic oscillator wave functions) states in the region in question. That is $n = 3$ for the $N = 28$, Ni, and $N = 50$ regions; $n = 4$ for the Sn and $N = 82$ regions, and $n = 5$ for the Pb. For the calculations, X was considered as a fixed constant in each region and $\hbar\omega_0$ was defined in each region in terms of a representative value of the mass number A. This quantity was then found to have a value of about $X = 110A^{-1}$ in each of the regions considered. The actual parameters used will be indicated with the theoretical results.

C. Energy Levels in S.C.S. Nuclei

In this section and in the Appendix, we shall present figures and tables from which the reader may estimate the position of all of the calculated zero, one, and two quasi-particle states and the collective 2^+ state, and from which he may determine the calculated wave functions. In the case of Pb^{206} and Pb^{204}, all of the calculated levels will be explicitly shown to indicate how the two quasi-particle states labelled by their spins, j and j', and parity are broken up by the $P^{(2)}$ force according to the total angular momentum J of the resulting state. For other even-A nuclei only those excited states, aside from the collective 2^+ state, which correspond to two identical quasi-particles will be indicated, and the breakup of the degeneracy

by $P^{(2)}$ obtainable from (18)—(21) will not be shown. From such a figure, the positions of the other excited states corresponding to two different quasi-particles can be obtained, aside from the effect of $P^{(2)}$, as the mid-point between the two excited states corresponding to pairs of quasi-particles of the two types (cf. Eq. (10)). This procedure is indicated in the figures for Pb^{206} and Pb^{204}. For the odd-A isotopes all of the one quasi-particle states are indicated. These are each non-degenerate levels aside from the m degeneracy of the quasi-particle angular momentum, $J = j$.

1. Pb Isotopes

The energy levels in Pb^{207} define the neutron hole well quite accurately. Since the experimental single-particle levels are known for the entire 82—126 neutron shell, this region should be a good one for our methods.

One also knows the positions of some of the particle levels in the next shell from Pb^{207}. Since these are unimportant in Pb^{206}, and grow even less important as the number of neutron holes in the 126 shell is increased, they serve only to renormalize G in our calculation.

The one disadvantageous feature for the Pb isotopes is that the first hole level has spin 1/2. For this reason, in the two-hole calculation, Pb^{206}, the lowest excited state is one with two quasi-particles of angular momentum 1/2, which is simply a 0^+ state. For reasonable magnitudes of G, this state seems to be almost entirely spurious, and must therefore be ignored.

In the odd-A Pb isotopes the main systematic experimental feature is the position of the $i_{13/2}$ state, which has been determined by a study of the $M4$ isomeric transition to the $f_{5/2}$ state.[19] For any reasonable strength of the pairing force, G, we obtain the correct position for this level. It is generally true that, although the absolute energies depend on the size of G in odd-A nuclei, the relative positions of the one quasi-particle levels are not very sensitive to the strength of the pairing force or the $P^{(2)}$ force, but depend mainly on the positions of the single-particle levels for any G which is consistent with the gap.

All of the experimental odd-A Pb ground states are found within 0.1 Mev, as can be seen in Fig. 1. In Pb^{205}, the theoretical $(1/2)^-$ state is below the $(5/2)^-$ state by about 0.05 Mev, while experiment gives the ground state spin as $(5/2)^-$,[20]; and the $(5/2)^-$ state might rise a little fast, since it is above the $(3/2)^-$ state by about 0.1 Mev in Pb^{197}, while rather uncertain experimental results give $(5/2)^-$ as the ground state spin. Such small deviations can easily be explained by the uncertainties expected in the calculations, especially by the presence of other perturbations besides the $P^{(2)}$.
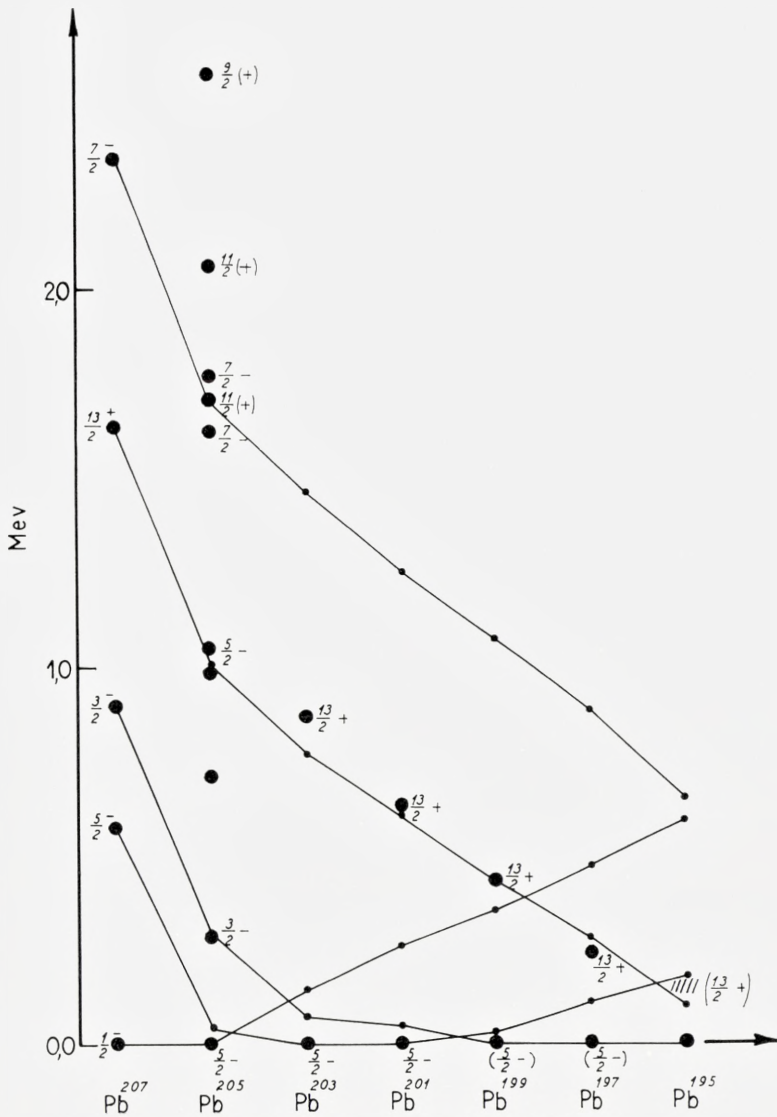
Fig. 1. *Energy levels of the odd-A* Pb *isotopes.*

The experimental points are large dots with spin and parity assignments placed on the right when known. The theoretical results are the small dots joined by solid lines giving the positions of the one quasi-particle states for $G = 23/A$ and $X = 0.4$. The effect of the coupling of the quasi-particle to the collective oscillation is included by Eq. (40) for the lowest few states. The labels on the experimental curves are the angular momenta of the one quasi-particle states. The experimental values are taken from BERGSTRÖM and ANDERSSON,[19] the table of STROMINGER, HOLLANDER and SEABORG, and the work of DŽELEPOW and PEKER[21]).

Above about 0.8 Mev a number of other states are arising from the phonons which have not been indicated in the figure. We seem to predict a $(3/2)^-$ ground state in Pb^{195} and the presence of low lying $(3/2)^-$ and $(1/2)^-$ states in Pb^{203} and Pb^{201}.

In the even-A Pb isotopes the position of the 2^+ level is known down to Pb^{200}. Using $G \approx 0.1$ Mev, this energy level is predicted quite well as the lowest two quasi-particle level which can give rise to a 2^+ level. However, the $B(E2)$ for this state in Pb^{206} is four times the single-particle value[22], suggesting that the intrinsic states lie somewhat higher and that the 2^+ state is collective. The position of the 2^+ level as a function of A and the value of the $B(E2)$ in Pb^{206} are accurately predicted. (Cf. § VII). However, of all of the s.c.s. nuclei, perhaps in Pb is the collective treatment of the 2^+ state least well justified. The 2^+ level and the levels corresponding to two identical quasi-particles appear together with some of the experimental levels in Fig. 2. Fig. 3 shows how the calculated levels vary as a function of G.

The positions of all of the zero and two-quasi-particle levels are shown in Figs. 4 and 5 for Pb^{206} and Pb^{204}, together with the experimental values. The agreement with experiment for Pb^{206} is, as expected, not as good as the results of TRUE and FORD.[13] However, all of the experimental levels with measured spins can be matched with quasi-particle levels to within a few tenths of one Mev, except for the lowest 2^+ level for which the collective treatment gives the correct energy. It must be pointed out that our treatment, which introduces the collective 2^+ level and retains as higher excited states all of the $J = 2$ two quasi-particle states as effected by $P^{(2)}$ in perturbation theory, contains a spurious 2^+ two quasi-particle state analogous to the spurious 0^+ two quasi-particle state of the Belyaev solution of the pairing Hamiltonian. Thus, in Figures 4 and 5, there is one extra 0^+ and one extra 2^+ state. In our case as in that of Ref. 13, the ground state of Pb^{206} is mostly $(p_{1/2})^2 \, J = 0$ so that the state composed of two $p_{1/2}$ quasi-particles is mostly spurious, the other two quasi-particle spin zero states being mostly real. On the other hand, the lowest 2^+ state of Ref. 13 and likewise our collective 2^+ state have large contributions from $(p_{1/2} \, f_{5/2})$ and $(p_{1/2} \, p_{3/2})$ and lesser contributions from several other configurations, so that, with our method of calculating, the spurious character is spread over several of the low lying 2^+ two quasi-particle states.

For $G = 0.128$ which is chosen so as to fit the position of the 9^- level in Pb ^{204}, and which is consistent with the data for Pb^{206}, one predicts the energy of the 9^- level in Pb^{202} to be 2.09 as compared with the experimental
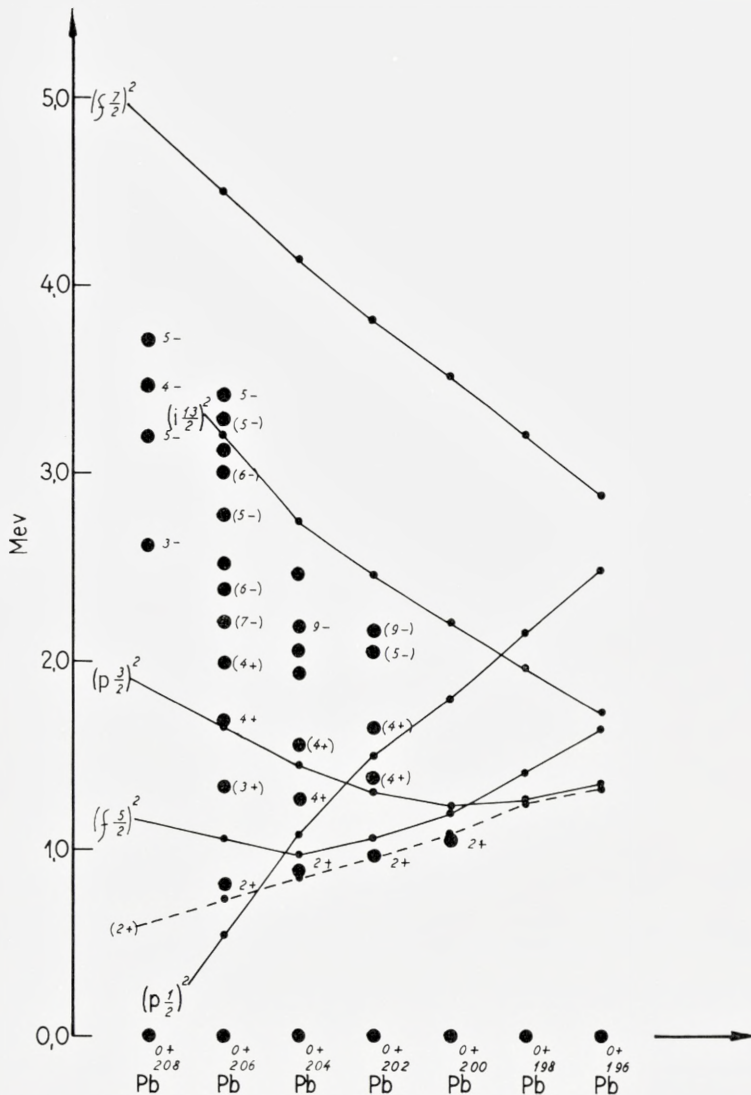
Fig. 2. *Energy levels of even-A Pb isotopes.*

The experimental points are large dots with spin and parity assignments placed on the right when known. The theoretical points are indicated by small dots. Those theoretical points which are joined by solid lines are the two identical quasi-particle states for $G = 23/A$ and are labelled to the left by the angular momenta of the quasi-particles. The effect of the $P^{(2)}$ force is not included for these states. The other two quasi-particle energies are found by taking the average energy between the appropriate two levels (see Figures 4 and 5). The collective 2^+ theoretical level is shown by small dots joined by a dashed line. The experimental values are taken from the table of STROMINGER, HOLLANDER and SEABORG and the work of DŽELEPOW and PEKER[21]). $X = 0.4$.
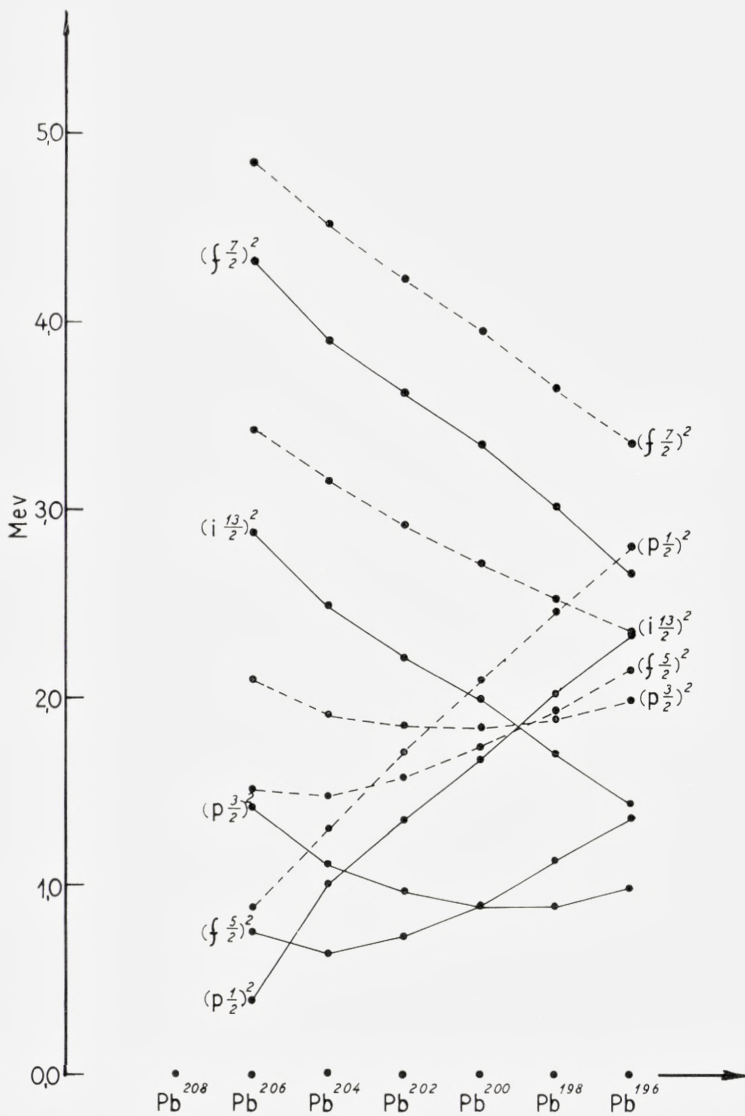
Fig. 3a.

Fig. 3. *Theoretical energy levels in even- and odd-A* Pb *isotopes as a function of* G.

The notation is that of Figs. 1 and 2. Only the zero and two identical quasi-particle states are given for the even-A isotopes and the one quasi-particle states for the odd-A isotopes. The solid lines are for $G = 0.0911$ and the dashed line for $G = 0.145$.
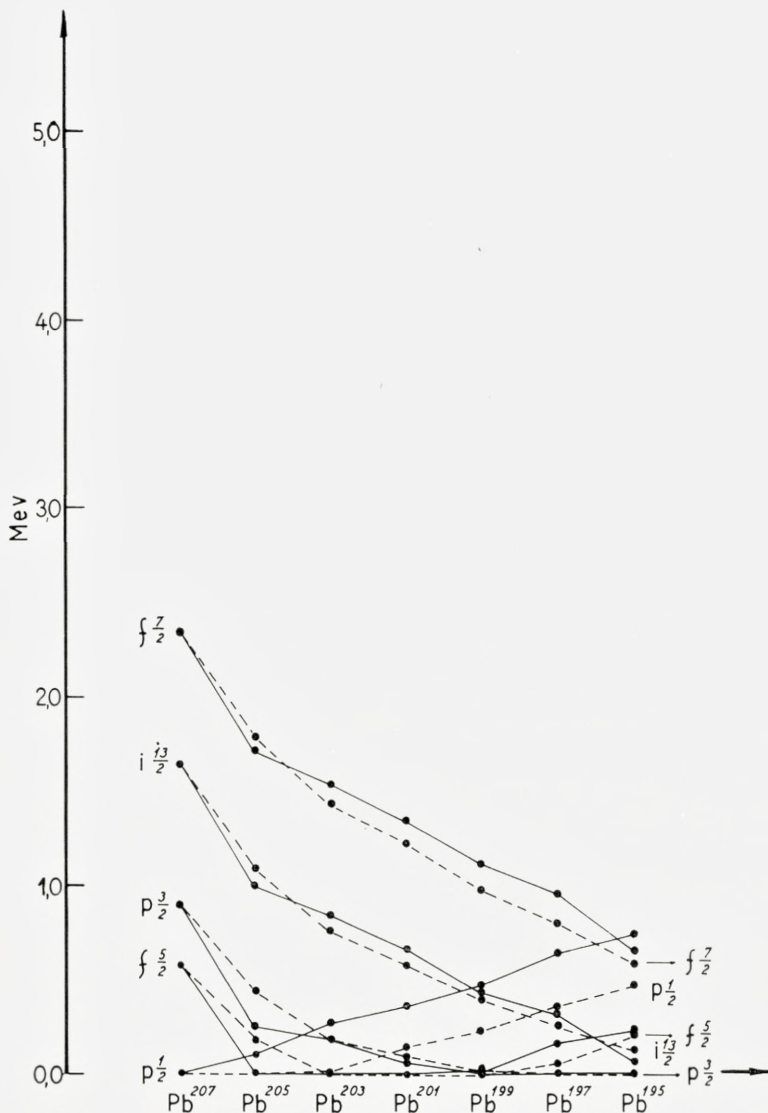
Fig. 3 b.

value of 2.171. The long lifetime of this level shows that it must lie below the near lying 6^-, 7^-, and 8^- levels. The $P_{22}^{(2)}$ force puts the 9^- below these other states coming from $(f_{5/2}\, i_{13/2})$, but the $(p_{1/2}\, i_{13/2})$ 6^-, 7^- quasi-particle states lie well below the 9^- in Pb^{206}, close in Pb^{204}, and above
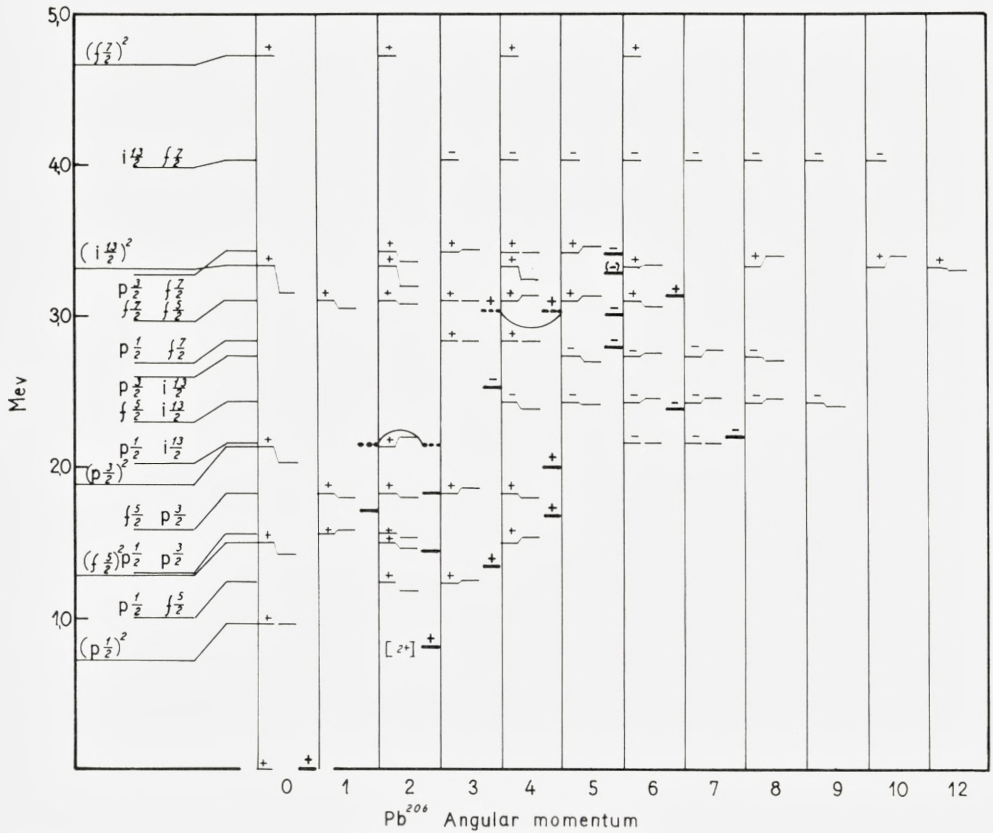
Fig. 4. *Energy levels of* Pb^{206}.

The experimental levels, taken from TRUE and FORD[13]), are given on the right for each spin. On the left for each spin for $G = 0.128$ is the two quasi-particle state perturbed by $\mathfrak{P}_{11}^{(2)}$ and Eq. (20) (see text), the labelled unperturbed states being given to the left of the diagram. The second column for each spin also includes the effect of $\mathfrak{P}_{22}^{(2)}$. The lowest 2^+ level, marked $[2^+]$, is the collective level. The state $(P_{1/2})_{J=0}^2$ is mostly spurious and there is one spurious state among the low lying 2^+ quasi-particle states. The $\mathfrak{P}_{22}^{(2)}$ effect is omitted in the highest states. $X = 0.4$.

in Pb^{202}. Thus, we can understand why this long-lived 9$^-$ state is seen in Pb^{202}, and Pb^{204}, but not in Pb^{206}.

2. *Sn Isotopes*

In the odd-A Sn isotopes nine ground states are known. In addition, systematic information about the $(11/2)^- - (3/2)^+$ separation is obtained from the isomeric $M4$ transition, and several excited states are known in Sn^{117}.
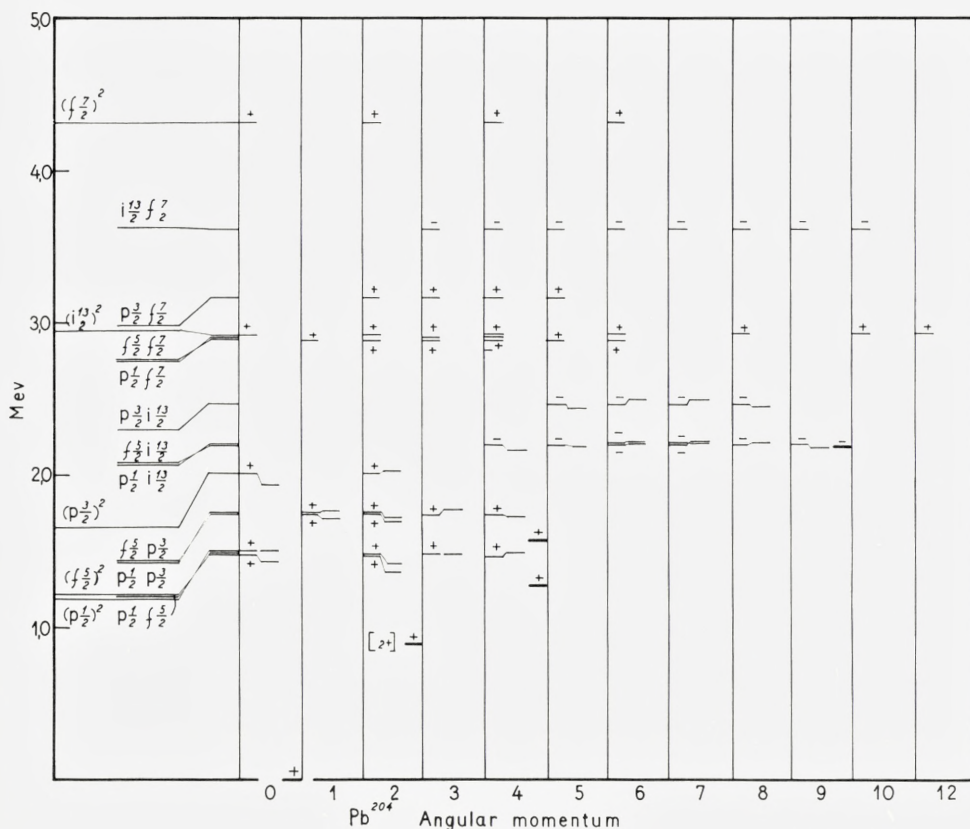
Fig. 5. *Energy levels of Pb²⁰⁴.*

The notation is the same as in Fig. 4. The spurious character is spread over several of the low lying 0^+ states in this case.

Of course, Sn^{101} is far from the stability curve, so the single-particle well cannot be obtained directly from experiment. One can learn something about the $(11/2)^- - (3/2)^+$ separation from the isotopes with 81 neutrons and even numbers of protons ($^{52}Te_{81}^{133}$, $^{54}Xe_{81}^{135}$, $^{56}Ba_{81}^{137}$, and $^{58}Ce_{81}^{139}$). However, one has a hard time to place the $(1/2)^+$ state correctly with respect to these two states and the separation between the $5/2$, $7/2$ states and the $1/2$, $3/2$, $11/2$ states is not known very well.

We tried calculations with several values of the single-particle energies. Although it is possible to choose a well which gives better results, the results using the well of S. G. NILSSON[11] are presented in Fig. 6. All of the important features which are known experimentally fit well (to about
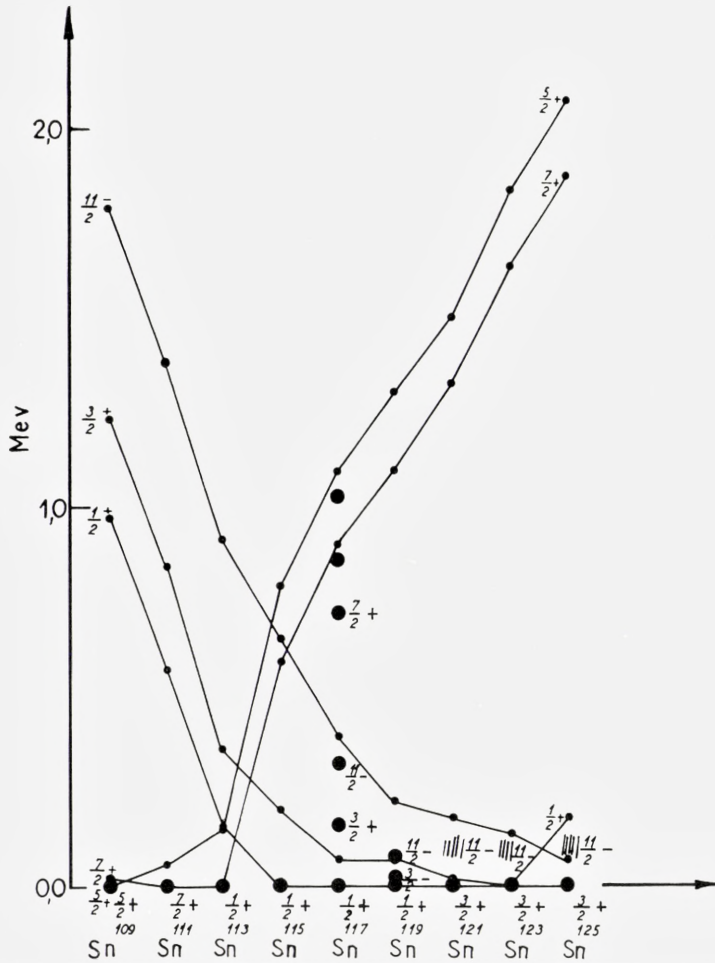
Fig. 6. *Energy levels of the odd-A Sn isotopes.*

The notation is the same as in Fig. 1, with $G = 19/A$ and $X = 1.1$. The single-particle levels are taken as $f_{5/2}$ (0); $g_{7/2}$ (0.22); $S_{1/2}$ (1.9); $d_{3/2}$ (2.20); $h_{11/2}$ (2.8 Mev).

0.1 Mev). One should notice that the 1/2 state remains the ground state as A changes by six. This feature depends not only upon the pairing force, but also upon the $P^{(2)}$ force. Also the $P^{(2)}$ force is important for keeping $(3/2)^+$ the ground state spin in Sn 123 and 125, for without it the $(11/2)^-$ would be the ground state, contrary to experiment.

For the even-A Sn isotopes shown in Fig. 7 the 7^- state in Sn^{120}, coming almost entirely from the two-quasi-particle state with one $(11/2)^-$ and
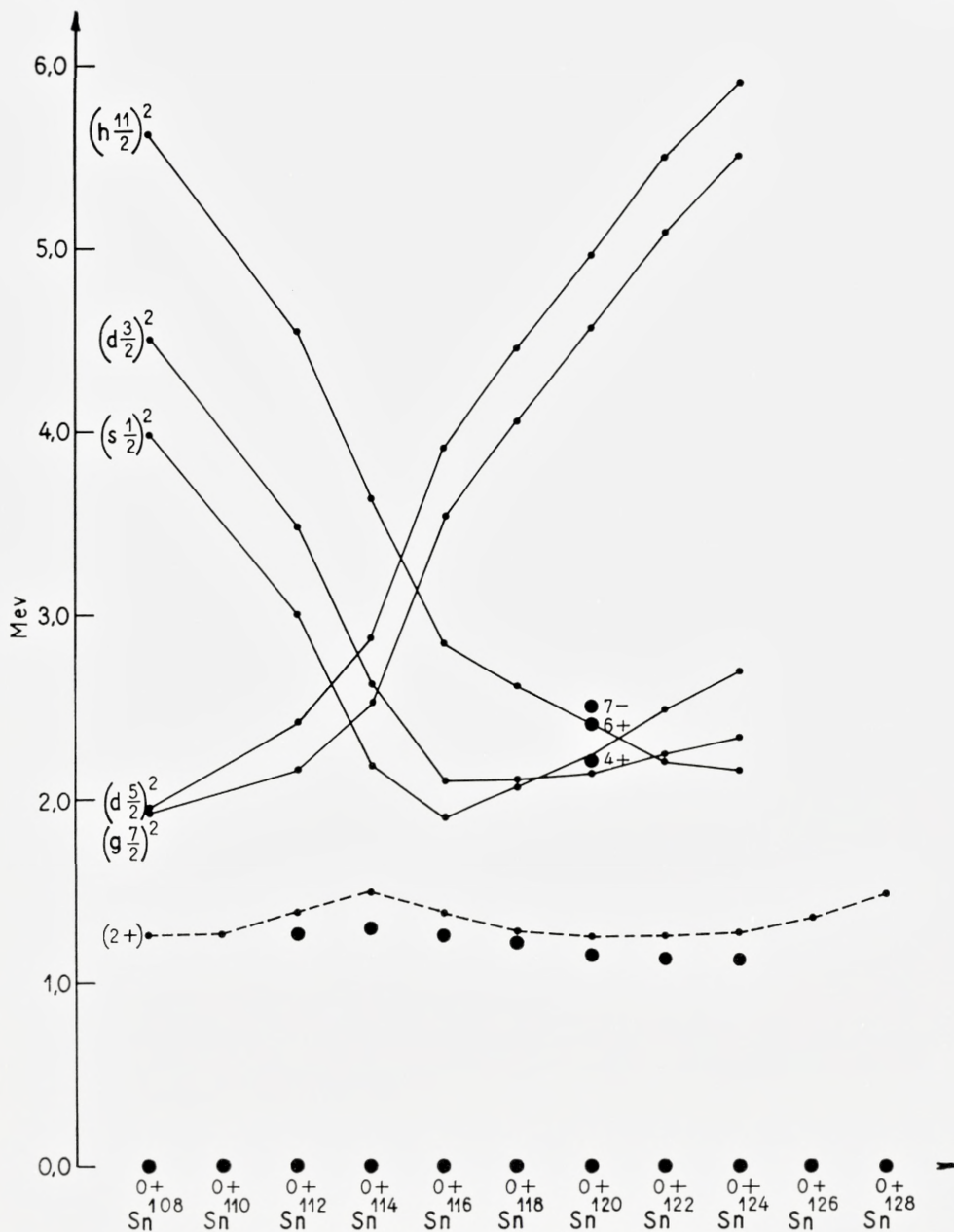
Fig. 7. *Energy levels of the even-A Sn isotopes.*
The notation is the same as in Fig. 2, with $G = 19/A$ and $X = 1.1$; and the single-particle energies are given in Fig. 6.

one $(3/2)^+$ quasi-particle, is moved little by the long range force. It is fit quite well by $G = 0.187$, corresponding to 0.0911 in Pb $(G = 19/A)$. The 6^+ state from two $(11/2)^-$ quasi-particles is also fit well, falling about 0.1 Mev below the 7^- level when $\mathfrak{P}_{11}^{(2)}$ and $\mathfrak{P}_{20}^{(2)}$ are included by (18), (19), and (20).

However, the important experimental results for the even-A Sn isotopes are the 2^+ states. There is a maximum in the $2^+ - 0^+$ energy separation at Sn^{114}.[23] This feature is fit in quite good detail by the collective state which occurs for the $G = 0.187$. In this case, the higher values of G will give rise to collective 2^+ states which will not fit the experimental values very well. Thus the combination of the 7^- and 6^+ states in Sn^{120} and the detailed experimental results for the 2^+ state serve to pick the value of G accurately as $19/A$.

3. Ni Isotopes

Since the levels in Ni^{57} are not known we must again use indirect evidence to find the well. For the neutrons moving in the 28—50 shell, the $p_{3/2} - p_{1/2}$ separation is known rather well from the magnitude of the spin orbit interaction. One needs to know, in addition, the position of the $(9/2)^+$ and the $(5/2)^-$ levels with respect to the p levels.

The $(9/2)^+ - (1/2)^-$ separation can be estimated from the isotopes with 49 neutrons and even numbers of protons. The pairing-force calculation is insensitive to this, since the $(9/2)^+$ state does not play a very important role in the Ni isotopes. However, the position of the $(5/2)^-$ level is quite important. Fig. 8 shows a sample calculation of how the levels in $_{26}Fe_{29}^{55}$ can give some information about this level. However the well of S. G. Nilsson[16] seems adequate for these isotopes, in spite of the apparent inconsistency of the $(9/2)^+ - (1/2)^-$ separation with experimental data.

Choosing the energy levels for the neutrons from ref. 13, we carry out the pairing force plus $P^{(2)}$ calculation. The results are shown in Figs. 9 and 10. The calculated ground state spins in the odd-A isotopes all agree with experiment to within 0.1 Mev. The motion of the 2^+ first excited state in the even-A Ni isotopes is best fit by the $G = 19/A$.

4. N = 82

There are experimental results for isotopes with 82 neutrons, for protons in the 50—82 shell from $_{52}Te^{134}$ to $_{64}Gd^{146}$. For all these isotopes, most of
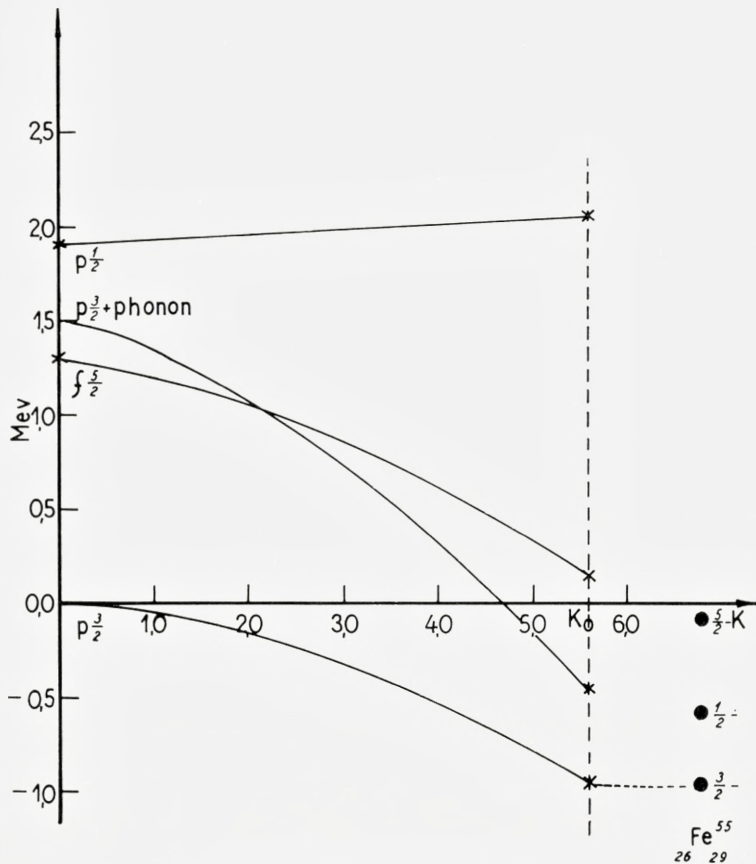
Fig. 8. *Energy levels of* $_{26}Fe^{55}_{29}$.

K is the strength of the coupling of the single-neutron states to the collective proton vibration. At $K = 0$, one has the assumed single-particle levels plus a phonon at 1.5 Mev. For $K = K_0$, the value of K is estimated from $_{26}Fe^{54}_{28}$, $_{26}Fe^{56}_{30}$, and $_{28}Ni^{58}_{30}$, the results are compared to the experimental values for Fe^{55}, which are given as large dots with energies to the right. The $p_{3/2}$ + phonon state which is given in the figure is the one with $J = 1/2$.

the extra-core protons are in the $(7/2)^+$ and $(5/2)^+$ levels. Therefore, only the separation of these levels need be known very well, especially since the 1/2, 3/2, 11/2 states are well separated from these levels. We use a separation of 1 Mev for the protons between the $(5/2)^+$ and $(7/2)^+$ states, which seems to be consistent with the levels in $_{51}Sb^{72}$ and $_{51}Sb^{74}$. The three higher states are taken as one state of pair degeneracy nine at 2.0 Mev.
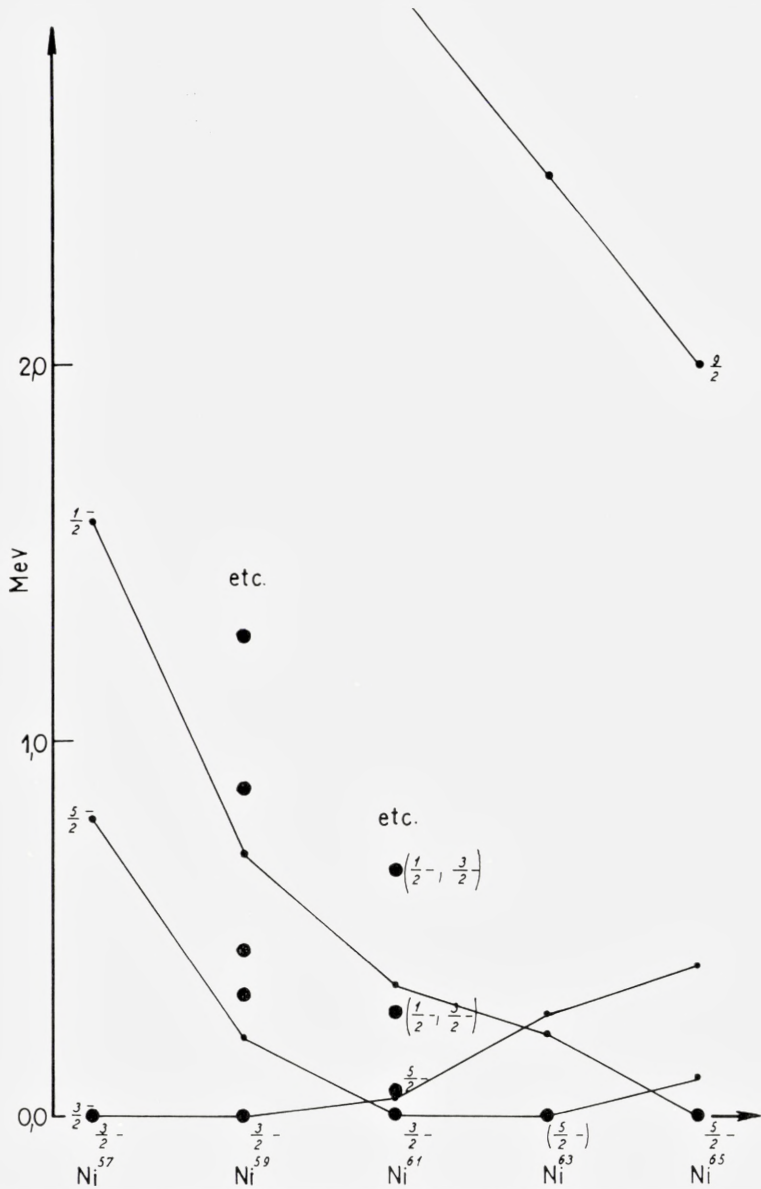
Fig. 9. *Energy levels of odd-A Ni isotopes.*

The notation is the same as in Fig. 1 with $G = 19/A$ and $X = 1.85$. The single-particle energy levels are

$$p_{3/2}\,(0);\; f_{5/2}\,(0.73);\; p_{1/2}\,(1.56), \text{ and } g_{9/2}\,(4.52 \text{ Mev}).$$
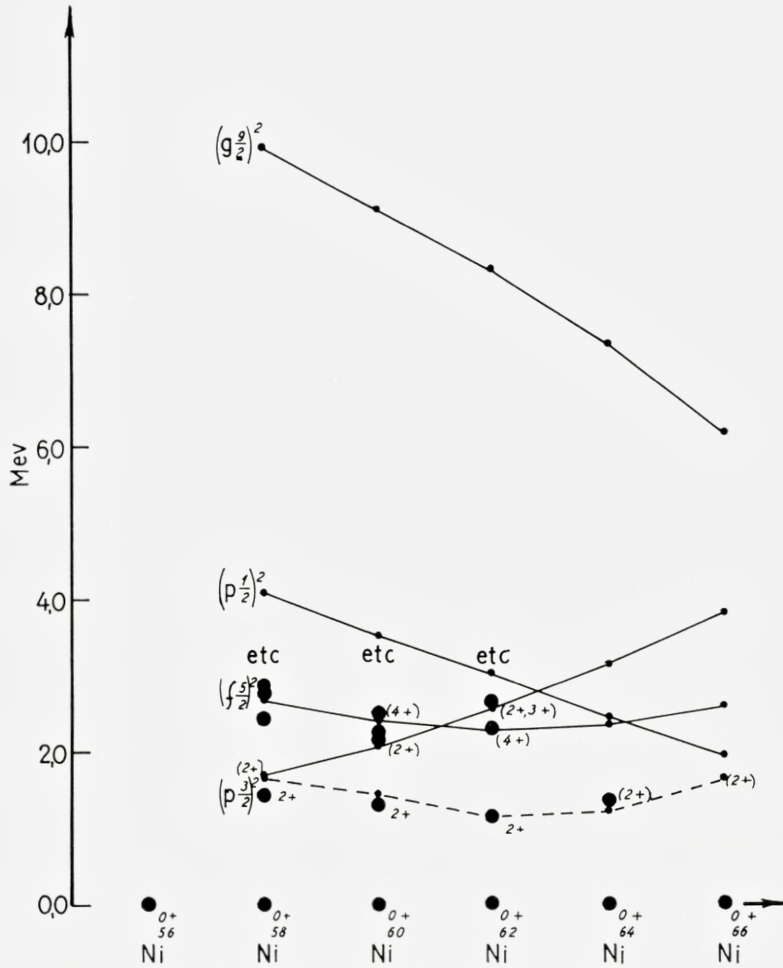
Fig. 10. *Energy levels of even-A Ni isotopes.*

The notation is the same as in Fig. 2 with $G = 19/A$, $X = 1.85$, and the single-particle levels of Fig. 9.

Figs. 11 and 12 give the result of this calculation. For the odd-A nuclei the ground states are correctly determined, as are the only two excited levels whose spins are known, the 0.163 Mev, $(5/2)^+$ level in La^{139} and the 0.145 Mev, $(7/2)^+$ level in Pr^{141}.

In the even-A nuclei one finds that the 2^+ collective levels are well determined for $G = 23/A$.

Fig. 11. *Energy levels of odd-A isotopes for* $N = 82$.
The notation is the same as in Fig. 1. See the text for the discussion of the well. $G = 23/A$ and $X = 0.975$.

5. $N = 50$

The region with a closed shell of neutrons and various numbers of protons in the 28—50 shell is a poor one for our calculation for several reasons. The first difficulty is that of finding the proper well for one proton outside of the double closed shell, i.e., $_{29}Cu^{79}_{50}$. But just as important in this case seems to be the fact that the percentage change in A is so great before one is at the isotopes for which there is empirical information that the well seems to have changed quite a bit.

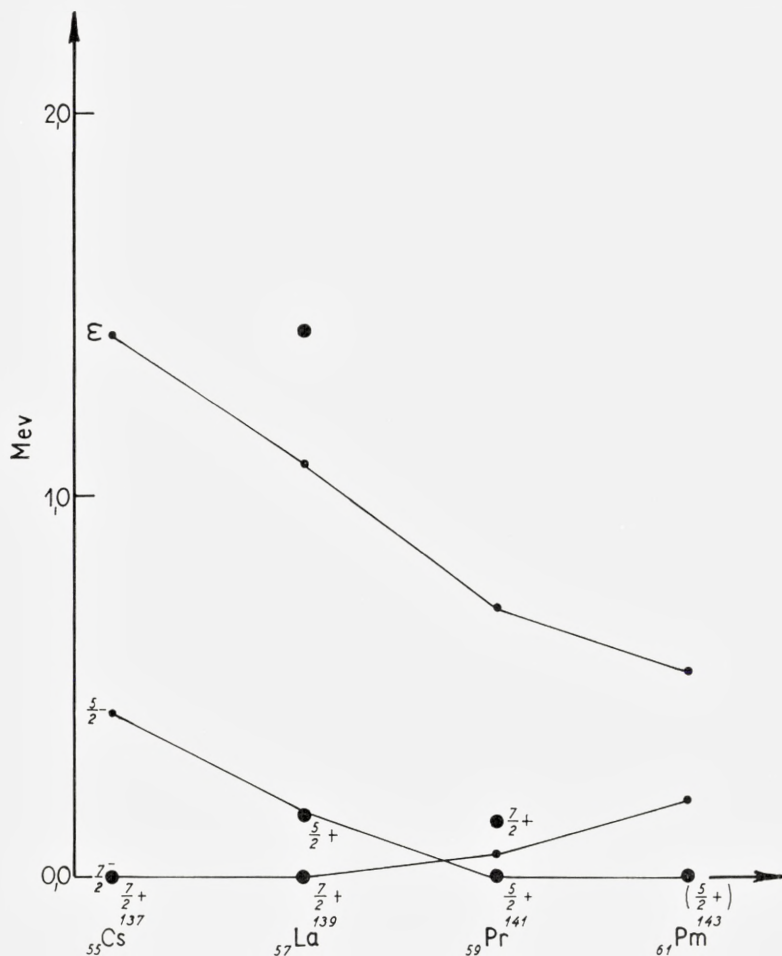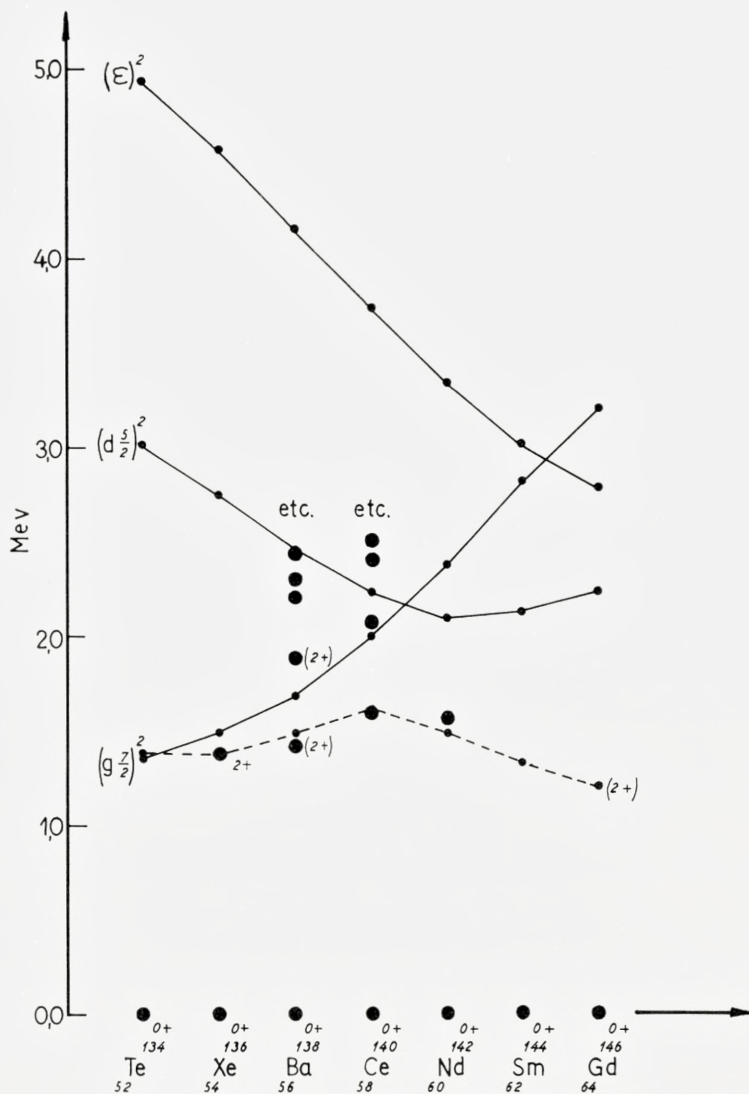Fig. 12. *Energy levels of even-A isotopes for* $N = 82$.

The notation is the same as in Fig. 2. See the text for the discussion of the well. $G = 23/A$ and $X = 0.975$.

Another characteristic of this region is that the Z's of the stable isotopes are just at the values for which the $p_{1/2}$ level is being filled. From the information we have, this level is rather separated from the other levels

Fig. 13. *Energy levels of odd-A isotopes for* $N = 50$.
The notation is the same as in Fig. 1. $G = 26/A$, $X = 1.22$, and the single-particle energy levels are
$f_{5/2}(0)$; $p_{3/2}(0.6)$; $p_{1/2}(1.8)$; $g_{9/2}(3.4 \text{ Mev})$.

of the shell. As explained in § II, such a situation can result in the Bardeen solution to the pairing force being very inaccurate.

A one-phonon intermediate coupling calculation is done, using the Cu levels to find the proton well in the same way as Fe^{55} is used to find the neutron well. This places the $p_{3/2}$, $f_{5/2}$, $p_{1/2}$ states in roughly the same positions for the single proton as the corresponding neutron states in the same
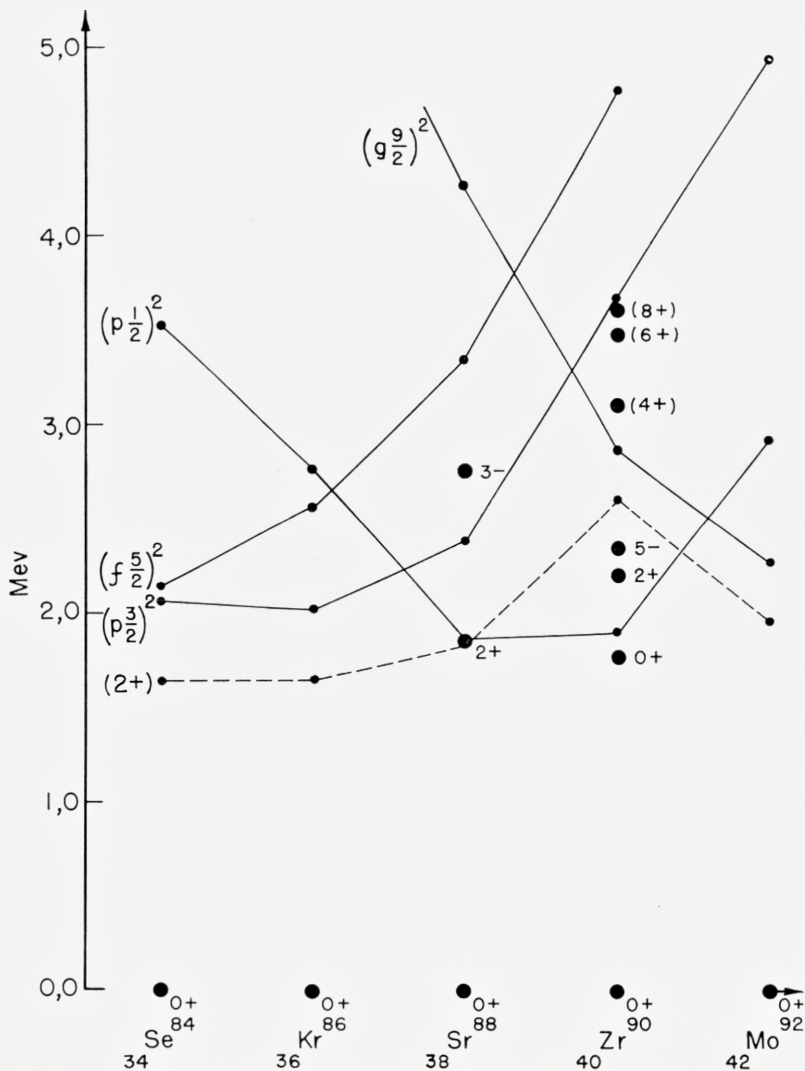
Fig. 14. *Energy levels of even-A isotopes for N = 50.*
The notation is the same as in Fig. 2 with G, X, and the well as in Fig. 13.

shell. One finds the $f_{5/2}$ state of the order of 1 Mev above the $p_{3/2}$ state. If this is the well for the protons, it is impossible to obtain the experimental $(3/2)^-$ ground states in $_{35}Br^{85}$ and $_{37}Rb^{87}$ with reasonable values of the G and χ parameters.
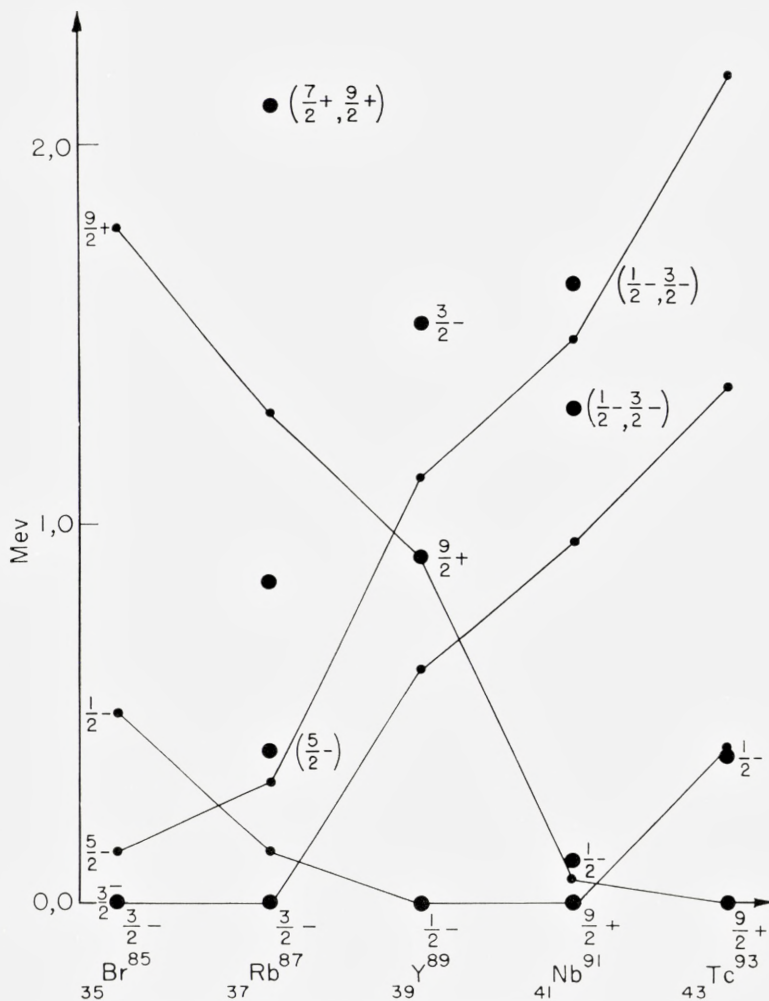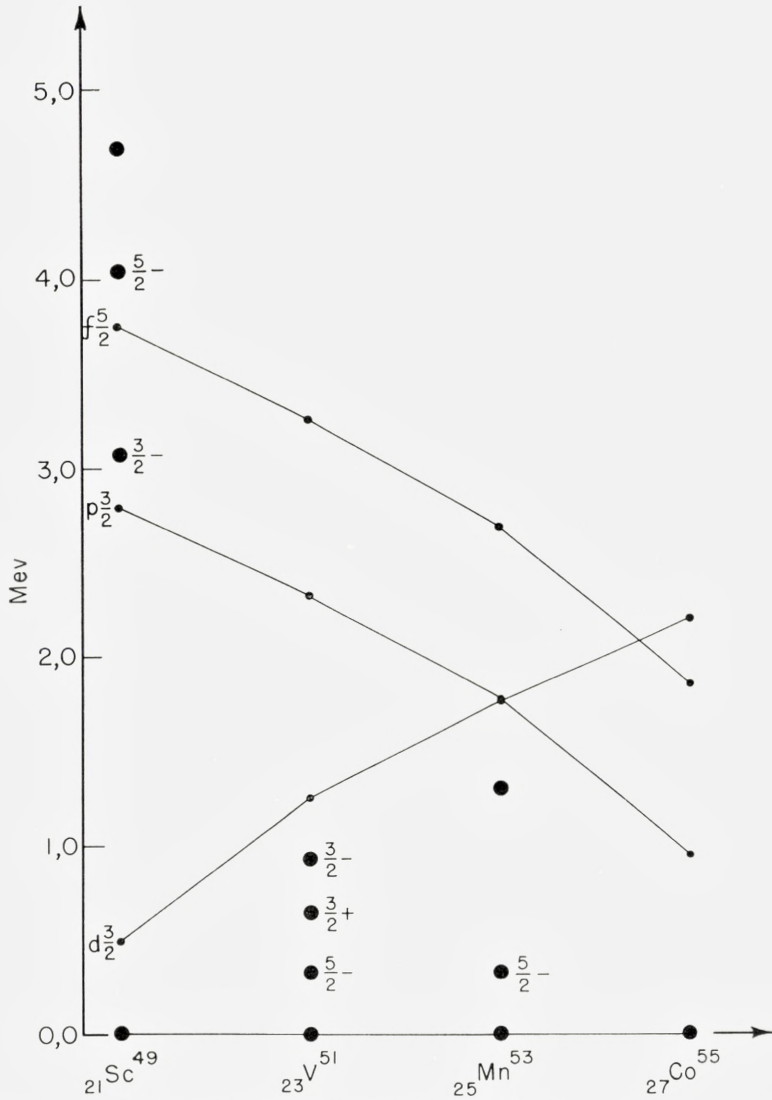
Fig. 15. *Energy levels of odd-A isotopes for* $N = 28$.

The notation is the same as in Fig. 1. $G = 19/A$, $X = 3.06$, and the single-particle levels are

$$d_{3/2}, \ (0); \ f_{7/2}, \ (2.5); \ p_{3/2}, \ (5.57); \ f_{5/2}, \ (6.54 \ \text{Mev}).$$

On the other hand, it is true that for the $N = 50$ isotopes the values of A are considerably larger than for the Cu isotopes used to determine the proton well. As one increases A, the spin orbit force decreases. It is possible
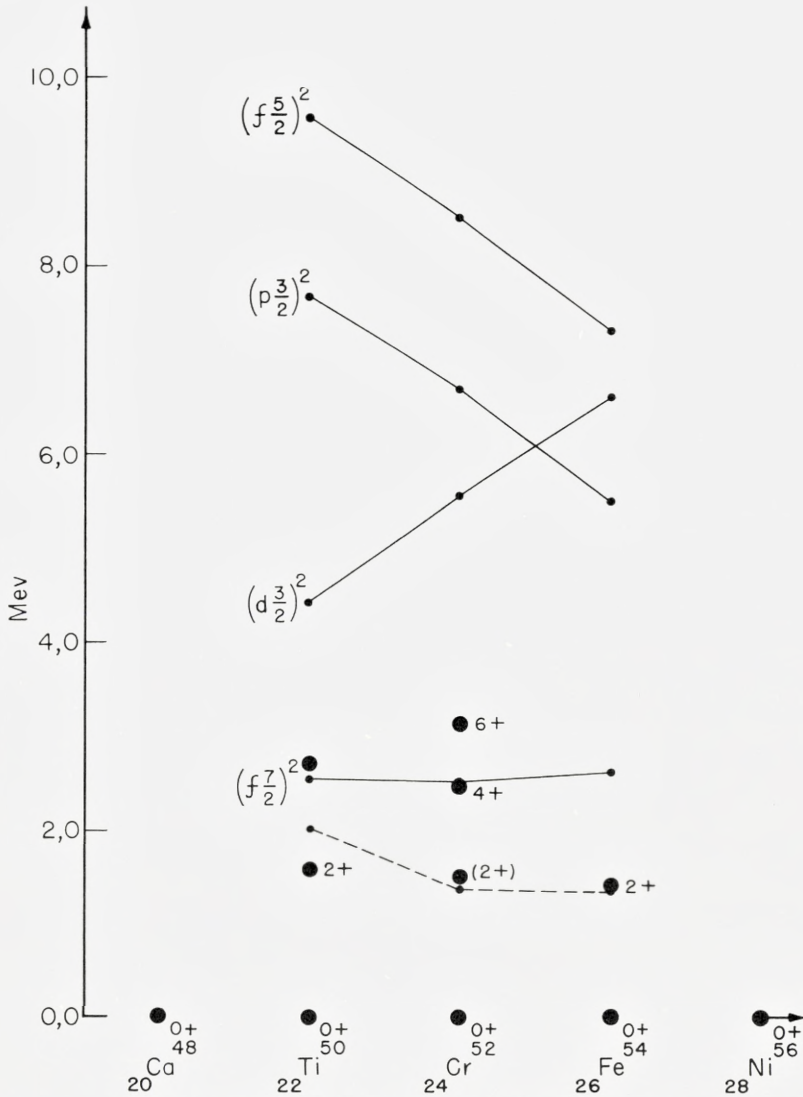
Fig. 16. *Energy levels of even-A isotopes for N = 28.*
The notation is the same as in Fig. 2 with G, X, and the well as in Fig. 15.

that the $f_{7/2}-f_{5/2}$ and $p_{3/2}-p_{1/2}$ separations have decreased so much as one goes from 63 to 85 that the $(5/2)^-$ state has come below the $(3/2)^-$ state. If one takes such a well, with a level ordering of $f_{5/2}$, $p_{3/2}$, $p_{1/2}$, $g_{9/2}$, it is possible to fit all of the odd-A $N = 50$ ground states as well as the known
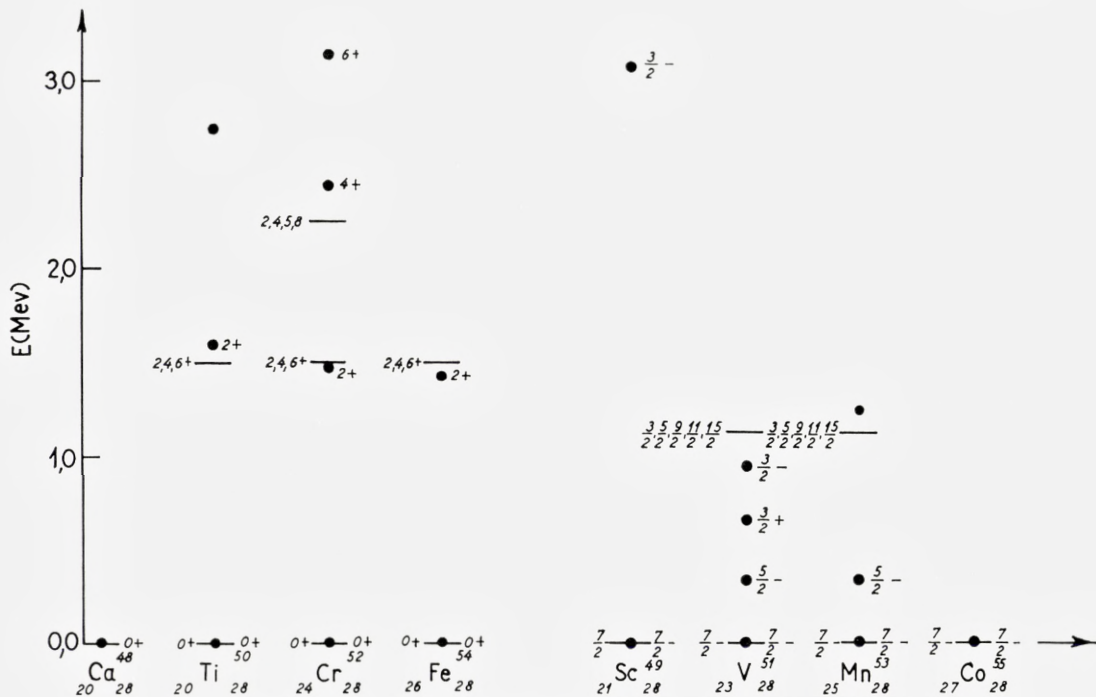
Fig. 17. *Exact diagonalization of pairing force for particles moving in a j = 7/2 shell compared with the experimental levels of the N = 28 isotopes.*

The experimental levels are indicated by dots with spin and parity assignments to the right and the theoretical levels by lines with the resultant angular momentum shown to the left of the line.

excited state information, within the accuracy of these methods, if the $(9/2)^+ - (1/2)^-$ separation is taken to be about 2.0 Mev and with $G = 26/A$. (Cf. Fig. 13).

For the even-A nuclei shown in Fig. 14 the most interesting feature is the low 0^+ excited state in $_{40}\mathrm{Zr}^{90}_{50}$. From our calculation we obtain a state of two quasi-particles of spin 1/2 about at this position for $G = 23/A$. As this state must be 0^+, this is a possible explanation for the experimental state. However, the state might be quite spurious, in which case the real lowest 0^+ excited state would be somewhat higher in energy for the same G. The $(9/2)^+ - (1/2)^-$ separation is critical in determining how spurious this state is. With only the levels in Sr[88] and Zr[90] it is difficult to draw much more information from these isotopes. Incidentally, if the 0^+ state is really associated with the two quasi-particle state, we would expect a

Fig. 18. Same as Fig. 17 except that in this case the force diagonalized is the sum of a pairing force plus a $P^{(2)}$ force of such relative strengths that the 0^+-2 separation of the even isotopes is produced by the combined results of the two parts of the force, the pairing force contributing two thirds and the $P^{(2)}$ force contributing one third to the separation.

0^+ state to lie near the 2^+ 1.85 Mev state in Sr^{88}. The most significant manner in which our Zr^{90} results differ from previous detailed calculations[24] is that the $f_{5/2}$, and especially the $p_{3/2}$, configurations are admixed, and seem to contribute to the low energy spectrum.

The results for both even-A and odd-A isotopes are quite sensitive to the choice of the single-particle levels in this region, and the results shown in Fig. 13 have been obtained only after several calculations with rather wide freedom in the choice of the single-particle values.

6. $N = 28$

Although $_{21}Sc_{28}^{49}$ experiments give the proton well for neutrons in a closed shell of 28, the region is still not a good one for our calculation. The small degeneracy of the levels in this region, i.e., $\Omega_{eff} \simeq 4$, leads to poor Bardeen solutions. The results of the calculation with a $G = 19/A$

Fig. 19. Same as Figs. 16 and 17, but with a relatively stronger $P^{(2)}$ force, the pairing force only contributing one third and the $P^{(2)}$ contributing two thirds to the 0^+-2^+ separation of the even isotopes.

and $P^{(2)}$ force are given in Figs. 15 and 16. Although the 2^+ state is fit pretty well as a collective state, the levels in the odd-A isotopes are not well fit. If the low lying odd parity excited states in $_{23}V^{51}$ and $_{25}Mn^{53}$ are to come from the single quasi-particle states corresponding to elementary excitations to levels in the next shell, such a large long range force perturbation will be needed to break down the seniority coupling scheme. Certainly, perturbation theory is inadequate for the long range force. The theoretical $(3/2)^+$ state listed in Fig. 15 is the one quasi-particle state associated with the $d_{3/2}$ level in the shell below.

We also performed an exact diagonalization of the pairing force plus $P^{(2)}$ force under the assumption of a degenerate $f_{7/2}$ level. Fig. 17, Fig. 18, and Fig. 19 give the results for three different combinations of G and $P^{(2)}$, all taken to fit the mean position of the 2^+ levels in the even-A nuclei. From these figures we see that it is possible to fit the experimental data for
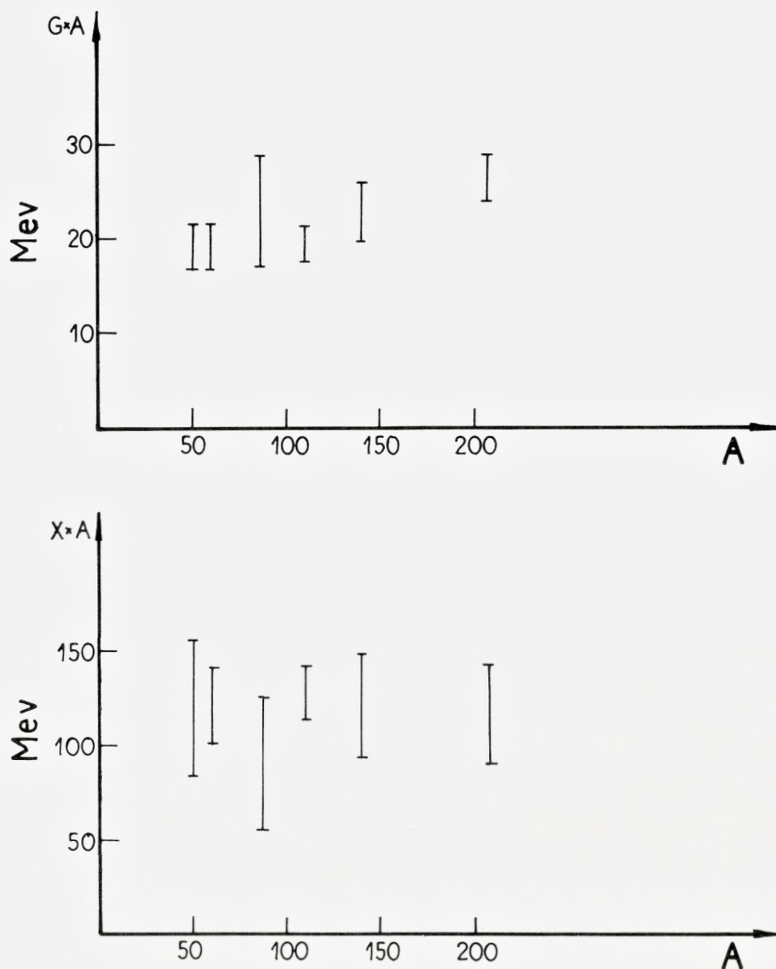
Fig. 20. *Coupling parameters.*

The coupling parameters used in each mass region are indicated. The vertical lines indicate the extent to which the magnitude of the parameters may be determined by fitting the experimental data.

the even-A isotopes and the low lying $(5/2)^-$ states in the odd-A isotopes with a pairing plus a $P^{(2)}$ force. The $(3/2)^+$ state in V^{51} presumably is associated with excitations from the shell below. If the $f_{5/2}$, $p_{3/2}$, and $p_{1/2}$ states from the next shell were included, one would obtain somewhat different results, and in particular the $(3/2)^-$ state might be lowered.

For regions lighter than $N = 28$, one would not expect our methods

to work very well. In these regions, the protons and neutrons are filling the same levels, so that the short range interaction between protons and neutrons becomes important to the extent that the particles in the closed shell are excited into the next higher shell. For example, there is evidence that the double closed shell of $N = Z = 20$ is not strong enough for our methods to be very accurate. Moreover, the effective pair degeneracy of the well becomes rather small. In conclusion, for the s.c.s. nuclei with $A \geq 49$, we fit the energy level systematics rather well with an approximate solution to the pairing plus $P^{(2)}$ residual force. Only in the $N = 50$ case does the change in the well with A in one region seem to give important effects. The two parameters, G and X, which are obtained as likely in each region are plotted in Fig. 20. From this it is seen that their A dependence is consistent with a volume force. This means that with only two parameters the low energy systematics for the intrinsic and 2^+ collective states of nuclei with one closed shell can be derived approximately.

IV. Total Binding Energies

A. Even-Odd Mass Differences

Assuming that an interacting shell model picture is a good one, the binding energies of nuclei can give information about the residual interaction. A systematic difference in the binding energies of even-odd and even-even nuclei is a direct consequence of the pairing force. The $P^{(2)}$ force, on the other hand, produces a ground state energy shift which, though large, has very little even-odd structure. Thus, a comparison between the experimental odd-even mass differences of the s.c.s. nuclei which we consider and the theoretical ground state energy differences between odd- and even-A nuclei can be used to help determine the magnitude of the pairing force constant G. We define the quantities P_n and P_p

$$P_n(Z, N) = E(Z, N) + E(Z, N-2) - 2E(Z, N-1), \qquad (42\,a)$$

$$P_p(Z, N) = E(Z, N) + E(Z-2, N) - 2E(Z-1, N), \qquad (42\,b)$$

where $E(Z, N)$ is the total binding energy of the nucleus, (Z, N). We consider P_n for Z closed and P_p for N closed. From (30) and (39) we see that, aside from the small shift due to the coupling of the quasi-particle to the
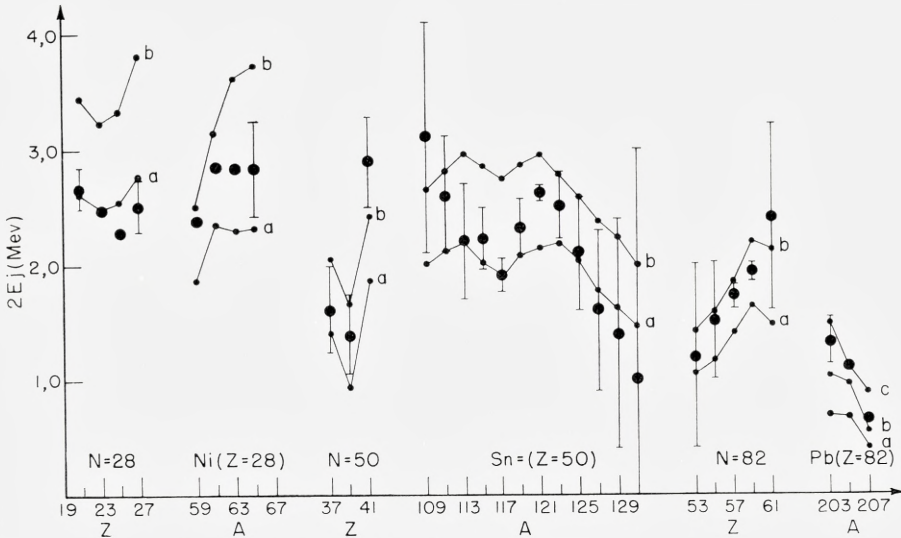
Fig. 21. *Even-odd-A mass difference.*

The P_n $(Z, N) = E$ $(Z, N) + E$ $(Z, N-2) - 2E$ $(Z, N-1)$ and P_p $(ZN) = E$ $(Z, N) + E$ $(Z-2, N) - 2E$ $(Z-1, N)$ are experimental quantities.[25] The theoretical curves are simply $2E_v$, twice the energy of the lowest lying quasi-particle for the odd-A isotope. Curves a and b correspond to $G = 19/A$ and $23/A$, respectively. Curve c (for lead only) corresponds to $G = 30/A$.

phonons, which we ignore, the odd-even-A difference given by P_n or P_p should just equal twice the energy of the odd-A quasi-particle, $2E_j$. In Fig. 21, the lines represent the quantity $2E_j$ for the ground state for various values of the coupling parameter G. The points are the experimental quantities P_n or P_p.

In each of the six pictured mass regions, the lower curve is the calculated mass difference value for $G = 19/A$, A being the representative mass number of the region. The next curve is for $G = 23/A$, and in the Pb region a third curve for $G = 30/A$ is included. The experimental points indicate that the data is consistent with the selected G values, but does not very strongly choose one over the other. Perhaps in the Pb region the two stronger values of G are preferred, while in the $N = 28$ region the lower value is better. This is in agreement with the energy level information discussed in the preceding section which indicates a preference for the value $G = 23/A$ in the Pb, $N = 82$, and $N = 50$ regions and the weaker $G = 19/A$ in the other regions.

4*

B. Absolute Binding Energies

In addition to the evidence for the gap, and therefore for the strength of the short range part of the residual shell model two-body interaction, the total binding energy data can give evidence for the absolute ground state energies of nuclei. Although the residual force employed in this work is certainly not the true force, it is hoped that in choosing a two-body interaction which gives the correct energy level spacing, one obtains the most important portions of the nuclear states. In particular, one would like to
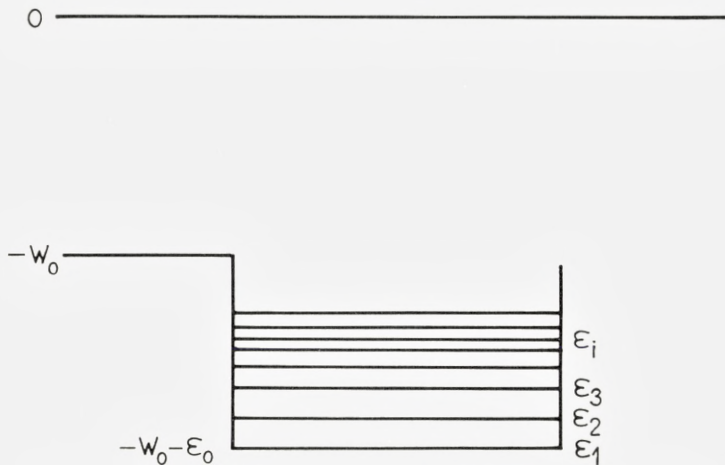
Fig. 22. *Energy diagram for non-interacting shell model particles.*

be able to calculate the total binding energy of the shell model particles outside of the closed shells.

In a particular region let us call the binding energy of the double closed shell nucleus W_0. Neglecting the Coulomb effect for the moment, if one adds one extra particle (or hole) it experiences an additional binding energy of ε_0 (cf. Fig. 22). The assumptions of this work imply that as more particles of the same type are added they fill the well defined by the isotope with one particle outside the double closed shells, so that, except for a possible gradual change with A of ε_0 and of the energies of the well, as well as of the binding energy of the core, W_0, the additional binding energy due to the outside particles is determined by single-particle energies, the two-body interaction, and the Coulomb force. Including the Coulomb force, the binding energy of the isotope with one particle outside the double closed shell is

$$W(1) = W_0 + \varepsilon_0 - (E_c^{(1)} - E_c^{(0)}), \tag{43}$$

where the Coulomb energy, E_c, is given by the Weizsäcker mass formula[26] as

$$E_c = 0.6 \frac{Z(Z-1)}{A^{1/3}} \text{ Mev.} \tag{44}$$

The binding energy of the isotope with n particles outside of the double closed shell is

$$W(n) = W_0 + \sum_{i=1}^{n} \left[\varepsilon_0 - (\varepsilon_i - \varepsilon_1) \right] - V_G(n) - V_L(n) - (E_c^{(n)} - E_c^{(0)}), \tag{45}$$

where V_G is the total interaction energy of the pairing force and V_L is the effect of the $P^{(2)}$ force in the ground state of the n particle system.

From Eqs. (9) and (45), one finds

$$-W(n) + W_0 + n\varepsilon_0 = U'(n) + V_L(n) + E_c^{(n)} - E_c^{(0)} \tag{46}$$

for an even-A nucleus, while

$$-W(n) + W_0 + n\varepsilon_0 = U'(n) + V_L(n) + E_c^{(n)} - E_c^{(0)} + \sqrt{(\varepsilon - \lambda)^2 + \Delta^2} \tag{47}$$

for an odd-A nucleus. In Eq. (47) the quasi-particle energy which appears is the smallest one for the isotope. It is difficult to know a priori the A dependence of ε_0 and W_0 or whether it should be the same for all regions. We make two calculations in each case, one holding ε_0 constant and the second giving ε_0 an $A^{-1/3}$ dependence. We use the average ε_0 as determined from adjacent nuclei.

The most favourable case to consider is that of the Pb isotopes, for here the experiments are accurate and one knows the binding energy of the double closed shell isotope, Pb^{208}, and the isotope with one hole in the neutron shell, Pb^{207}. From these one finds[27]

$$\varepsilon_0(Pb^{207}) = -7.357 \pm 0.043. \tag{48}$$

Using (48), one has accurate experimental values for $-W(n) + W_0 + n\varepsilon_0$ for Pb^{206} and Pb^{204}. In Fig. 23 these values are compared to the theoretical ones for $G = 0$, $G = 0.111$, and $G = 0.145$. One sees that both for ε_0 constant and for $\varepsilon_0 \sim A^{-1/3}$ the theoretical results are consistent with the data, and
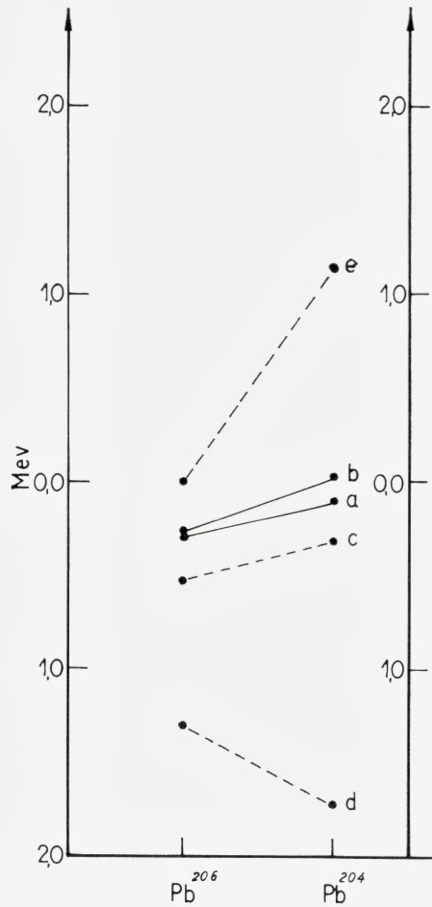
Fig. 23. *Absolute binding energies of the Pb isotopes.*
a and b are the experimental curves of $-W(n) + W_0 + n\varepsilon_0$ for ε_0 constant and $\varepsilon_0 \sim A^{-(1/3)}$, respect-
ively; c, d, and e are the theoretical curves for $U(n) + V_L(n)$ for $G = 0.111$, $G = 0.145$, and
$G = 0$, respectively. $\varepsilon_0 = -7.357$ from Pb[208] and Pb[207] experimental binding energies.[27]

the value of $G = $ about $23/A$ is favoured. This is consistent with the results
of the energy level calculation. However, the errors in the experimental
results are large enough to make this result somewhat uncertain.

For the Ni isotopes and for the $N = 82$ region, one is at the beginning
of a major shell. However, for neither of these series of isotopes is the binding
energy known for the double closed shell and the double closed shell plus
one nucleon isotopes. Therefore, one can merely determine if the results
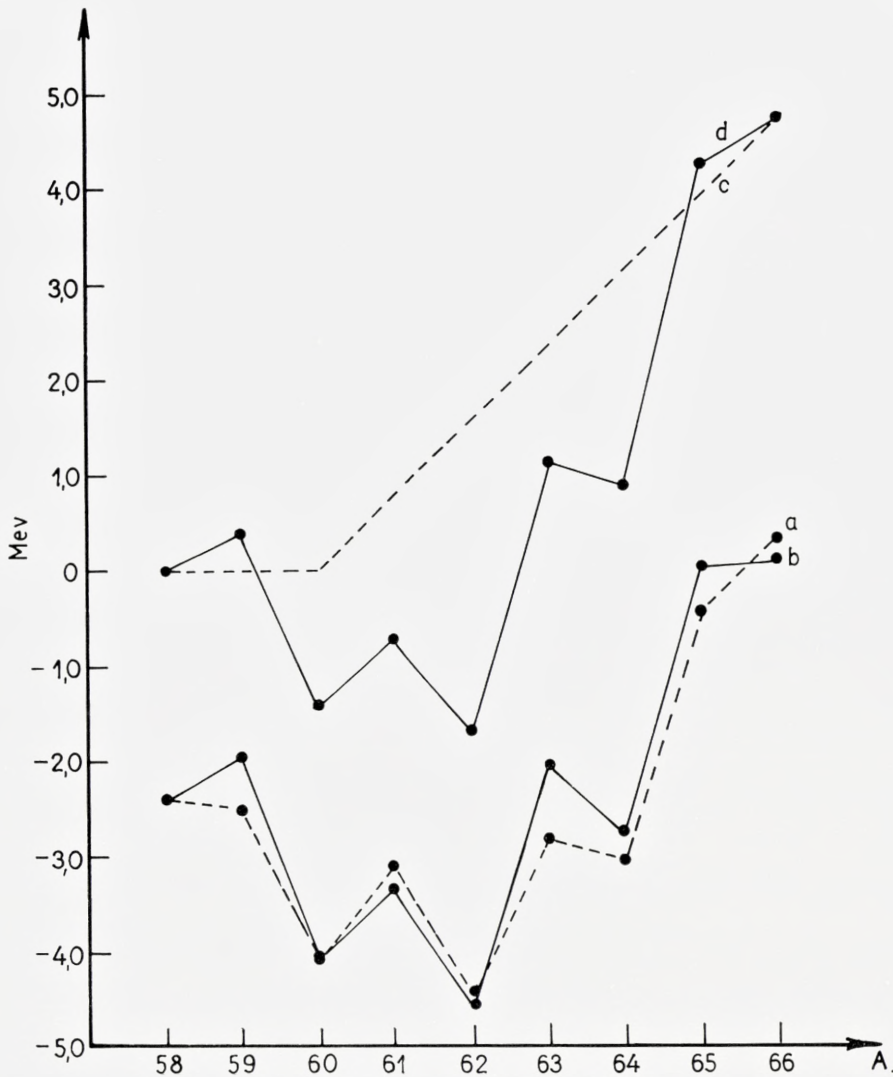
Fig. 24. *Binding energies of the Ni isotopes.*

a is the theoretical curve of $U'(n) + V_L(n)$ for $G = 19/A$, b is $-W(n) + W_0 + n\varepsilon_0$ with $\varepsilon_0 \sim A^{-(1/3)}$. The curves have been fit at Ni^{58}. Curves c and d are analogous to e and a of Fig. 23, respectively.

of the theoretical calculation are consistent with the known experimental results, and cannot experimentally determine the total binding energy of the n particles outside of the closed shells. However, the binding energy curves have considerable structure, reflecting the two-body force by a dip
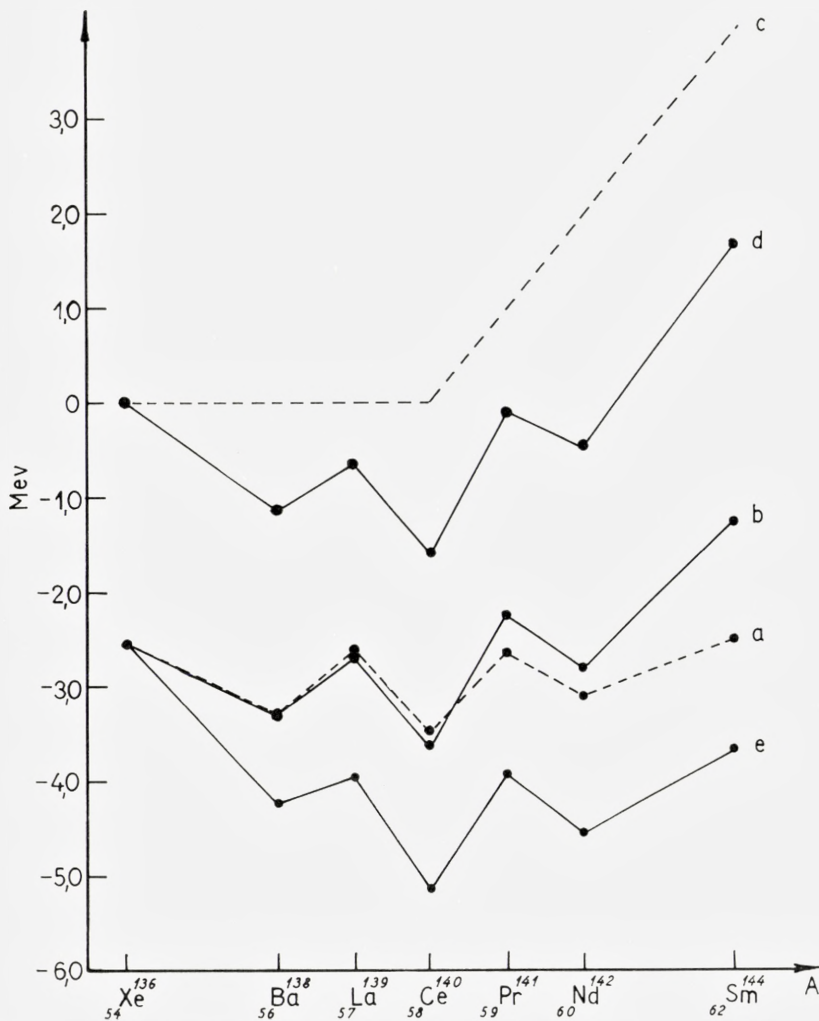
Fig. 25. *Binding energy of the N = 82 isotopes.*

a is the theoretical curve for $U(n) + V_L(n)$, *b* and *e* are the values of $-W(n) + W_0 + n\varepsilon_0$ for $\varepsilon_0 \sim A^{-(1/3)}$ and ε_0 constant, respectively; they are fit at $_{54}X_{82}^{136}$. Curves *c* and *d* are analogous to *a* and *e*, respectively, for $G = 0$.

in the $-W(n) + W_0 + n\varepsilon_0$ curve for the even-*A* and odd-*A* nuclei separately, as well as the even-odd mass difference (cf. Figs. 24 and 25). In both cases, after the experimental curves are normalized at the first point, the dip is quite well reproduced if $\varepsilon_0 \sim A^{-1/3}$, but the statistics do not rule out a constant ε_0.

The Sn isotopes are in the middle of a shell, forcing us once more to fit at one isotope; and there is very little structure to the curves except the rise of the Fermi level and the even-odd mass difference. For this reason we do not present the diagram. In this case the constant ε_0 seems to be favoured. Of course, these results depend upon the positions of the single-particle levels which are not too well known. The $N = 50$ region is also in the middle of a shell, so the total binding energy information is not so useful, since one must fit at one point.

In conclusion, we see that the total binding energy data is consistent with the theoretical results in every case. In addition, in the Pb region, the results can be used to help select the G which is most favourable. There is an indication that the well depth changes as $A^{-1/3}$ near closed shells and that it might have a slightly different A dependence in the middle of a shell than at the beginning or end. One should remember that there are rather large uncertainties in both the theoretical and emperical results which go into drawing these conclusions.

V. Electric Quadrupole Moments

For s.c.s. odd-A nuclei described by the collective Hamiltonian (39), the total quadrupole moment operator is the sum of the single-particle and collective operators

$$Q_0^T = \sum_{\nu\nu'}{}' q_{\nu\nu'}^0 \left(U_\nu U_{\nu'} - V_\nu V_{\nu'}\right)\left(\alpha_{\nu'}^\dagger \alpha_{\nu'} + \beta_{\nu'}^\dagger \beta_\nu\right) + Q_0. \tag{49}$$

The single-particle operator, $Q_{\text{s.p.}}$, of which we have only included the part diagonal in the number of quasi-particles, cannot change the number of collective quanta (phonons); and the collective operator changes the number of phonons by ± 1, but does not affect the quasi-particles. Thus $Q_{\text{s.p.}}$ contributes to the quadrupole moment in zeroth order perturbation theory, while the contribution from Q_0 first appears in a term proportional to χ. For a quasi-particle of angular momentum j, the single-particle moment is

$$\left.\begin{aligned}
Q_{\text{s.p.}} &= \sqrt{\frac{16\pi}{5}}\,\langle j \,|\, r^2 Y_0^2 \,|\, j\rangle_{m=j}\,(U_j^2 - V_j^2)\,e_{\text{eff}} \\[2mm]
&= +\frac{2j-1}{2(j+1)}\,\langle j \,|\, r^2 \,|\, j\rangle\,(U_j^2 - V_j^2)\,e_{\text{eff}}.
\end{aligned}\right\} \tag{50}$$

For the coupled system, making the same assumptions needed to obtain (34), we obtain for the collective moment contribution

$$Q_{\mathrm{coll}} = + \frac{2\,j-1}{2\,(j+1)} \langle j \,|\, r^2 \,|\, j \rangle \, (U_j^2 - V_j^2) \frac{\chi}{C} \, e_{\mathrm{eff}}, \tag{51}$$

so that the total quadrupole moment is given in perturbation theory by

$$Q = + \frac{2\,j-1}{2\,(j+1)} \langle j \,|\, r^2 \,|\, j \rangle \, (U_j^2 - V_j^2) \, e_{\mathrm{eff}} \left(1 + \frac{\chi}{C} \right). \tag{52}$$

Quadrupole moments are known experimentally for only four of the s.c.s. odd-A nuclei which we consider. The experimental and theoretical moments calculated, using G and χ which best fit other data, are shown in Table I. An effective charge of two units was used in the calculation.

TABLE I

Isotope	j	$\dfrac{\chi}{C}$	$(U^2 - V^2)$	Q theoretical $[10^{-24}\,\mathrm{cm}^2]$	Q experimental $(10^{-24}\,\mathrm{cm}^2)$
$_{57}\mathrm{La}^{139}$	7/2	1.2	$-.25$	$+.21$	$+.27$
$_{59}\mathrm{Pr}^{141}$	5/2	1.6	$.44$	$-.36$	$-.05$
$_{37}\mathrm{Rb}^{87}$	3/2	1.0	$-.47$	$+.15$	$+.14$
$_{23}\mathrm{V}^{51}$	7/2	2.2	$.25$	$-.17$	$+.03$

The table compares the experimental and theoretical electric quadrupole moments of s.c.s. nuclei, based on the coupled system of quasi-particle and quadrupole vibration.

It is seen that the La^{139} and Rb^{87} moments agree well with experiment. The theoretical moment of Pr^{141} is too large by a factor of 7, but this result could be improved considerably by the use of a different shell model well which would in turn alter particularly the quantity $(U^2 - V^2)$ in (52). However, it is difficult to see how the sign of the V^{51} moment could be changed within our model, for this would mean that, with only three protons beyond the twenty closed shell, the $f_{7/2}$ shell is effectively more than half filled. Including the $d_{3/2}$ levels below the shell in the calculation of the V's and U's does not seem to have a strong enough effect to cause this. The meager experimental data for the quadrupole moments of odd-A s.c.s. nuclei do not provide a detailed test of the nuclear wave functions. Thus, the question

remains open as to whether admixed configurations to the pairing force wave function other than those produced by the quadrupole field may also contribute significantly to the quadrupole moment. Also other authors have not succeeded in explaining the V^{51} moment by considering configuration mixing[28].

VI. Magnetic Dipole Moments in Odd Nuclei

A. Magnetic Moments with Pairing and $P^{(2)}$ Force Model

The magnetic moment operator for the coupled system of phonons and quasi-particles is the sum of the quasi-particle magnetic moment and that of the phonon. The quasi-particle magnetic moment operator is

$$\left.\begin{aligned} \hat{\mu}_{\text{s.p.}} &= \sum_{\nu\nu'} \langle \nu \,|\, \mu \,|\, \nu' \rangle \, (U_\nu U_{\nu'} + V_\nu V_{\nu'}) \, (\alpha^\dagger_\nu \alpha_{\nu'} - \beta^\dagger_{\nu'} \beta_\nu) \\ &+ \sum_{\nu\nu'} \langle \nu \,|\, \mu \,|\, \nu' \rangle \, (U_\nu V_{\nu'} - V_\nu U_{\nu'}) \, (\alpha^\dagger_\nu \beta^\dagger_{\nu'} - \beta_\nu \alpha_{\nu'}), \end{aligned}\right\} \quad (53)$$

where μ is the usual particle magnetic moment

$$\mu = j g_j = j\left(g_l \pm \frac{1}{2\,l+1}\,(g_s - g_l)\right); \quad j = l \pm \frac{1}{2}, \quad (54)$$

g_j is the total single-particle g-factor, and

$$g_s = \left\{\begin{aligned} 5.585 \\ -3.826 \end{aligned}\right\} \quad \text{and} \quad g_l = \left\{\begin{aligned} 1 \\ 0 \end{aligned}\right\} \quad (55)$$

for protons and neutrons, respectively. The only non-diagonal terms in (53) are those for which ν and ν' are spin orbit partners. It is seen from (53) that quasi-particles have the same magnetic moments as particles, since $(U^2 + V^2) = 1$. This is easily understood, since particles and the corresponding holes also have the same magnetic moments. The second term in (53) plays no role since the collective Hamiltonian (29) cannot change the number of quasi-particles. Thus, with only pairing forces, the odd-A nuclei will exhibit single-particle values (the Schmidt line values) for their magnetic moments.

The collective Hamiltonian (39) will lead to magnetic moments different from single-particle values by coupling the quasi-particle to a phonon and, of more importance, by admixing near lying quasi-particle states. For the

first and less important effect we must know the g-factor, g_R, for the phonon. This depends upon what part of the angular momentum of the collective 2^+ state comes from the protons and what part from the neutrons. Our model, in which the collective motion involves the extra-core particles together with the core (included as a renormalization effect), suggests a somewhat higher g-factor for extra-core proton than for extra-core neutron nuclei. However, for the calculations we have taken $g_R = 0.45$. The phonon magnetic moment operator is then $g_R R$, where R is the phonon angular momentum. Since neither the phonon nor quasi-particle magnetic moment operators can change the number of phonons, the shift of the magnetic moment from its single-particle value will first appear in perturbation theory in a term proportional to χ^2.

In the perturbation approximation one obtains[2] from the diagonal part of (53)

$$
\left.
\begin{aligned}
\mu = \mu_{\mathrm{s.p.}} + \frac{5}{16\pi} \frac{1}{j} \frac{\chi^2}{\hbar\omega C} \sum_{j'} \{ -\alpha_{jj'}(g_j - g_R) + \beta_{jj'}(g_{j'} - g_R) \} \\
\left(\frac{\hbar\omega}{\hbar\omega + E_{j'} - E_j} \right)^2 (U_j U_{j'} - V_j V_{j'})^2,
\end{aligned}
\right\} \quad (56)
$$

where $\alpha_{jj'}$ and $\beta_{jj'}$ are tabulated by Bohr and Mottelson (Table V, Ref. 2) or can be taken as

$$
\alpha_{jj'} = 2 \left(C^{2\,j\,j'}_{0\,\frac{1}{2}\,\frac{1}{2}} \right)^2 j^2 \tag{57 a}
$$

$$
\alpha_{jj'} - \beta_{jj'} = \left(C^{2\,j\,j'}_{0\,\frac{1}{2}\,\frac{1}{2}} \right)^2 \frac{j}{j+1} \left[j(j+1) - j'(j'+1) + 6 \right]. \tag{57 b}
$$

If quasi-particle states j', j'' which are spin orbit partners of each other appear in the one phonon amplitude, there is an additional contribution to μ from the non-diagonal part of (53). This additional contribution is

$$
\left.
\begin{aligned}
\delta\mu = \frac{5}{16\pi} \frac{1}{j} \frac{\chi^2}{\hbar\omega C} (g_s - g_l) 2\, C^{2\,j\,j'}_{0\,\frac{1}{2}\,\frac{1}{2}}\, C^{2\,j\,j''}_{0\,\frac{1}{2}\,\frac{1}{2}} \frac{j}{(j+1)(2\,l+1)} \\
\sqrt{\left(j + l - \frac{3}{2}\right)\left(j + l + \frac{7}{2}\right)} \cdot \sqrt{\left(l - j + \frac{5}{2}\right)\left(j - l + \frac{5}{2}\right)} \frac{\hbar\omega}{\hbar\omega + E_{j'} - E_j} \\
\frac{\hbar\omega}{\hbar\omega + E_{j''} - E_j} (U_\nu U_{\nu'} - V_\nu V_{\nu'})(U_\nu U_{\nu''} - V_\nu V_{\nu''})(U_{\nu'} U_{\nu''} + V_{\nu'} V_{\nu''}),
\end{aligned}
\right\} \quad (58)
$$

where

$$j' = l - \frac{1}{2}, \quad j'' = l + \frac{1}{2}. \tag{59}$$

For $j = j'$ or $j = j''$ this expression (without the U, V factor) is equivalent to IV. 8, Ref. 2. The other cases where these terms can contribute are when $j = j' - 1$ and $j = j'' + 1$.

Using (56) and (58) and the G and χ which best fit other data, we have calculated the shift of the magnetic moment from the Schmidt line for all s.c.s. nuclei for which the magnetic moments are known experimentally. The result is that, although the shift from the single-particle moment is always in the right direction, it is always too small by a factor of from four to ten. The reason for this is the factor $(U_\nu U_{\nu'} - V_\nu V_{\nu'})$, appearing in the collective Hamiltonian (39), which greatly weakens the coupling of the ground state to the collective vibration. Thus it does not seem to be possible to understand the shift of the quasi-particle magnetic moment of s.c.s. odd-A nuclei from the single-particle value on the basis of the coupling of the quasi-particle to the collective oscillations.[29]

B. Magnetic Moments with Configurations Admixed by a δ-Function Force

ARIMA and HORIE[30], and BLIN-STOYLE,[31] have pointed out that a small amount of mixing of certain kinds of configurations can produce large changes in the magnetic moments of nuclei, without changing appreciably the pure shell model configurations upon which they base their calculations.

From the results of Section A of this chapter it is clear that the configuration mixing produced by the long range part of the force is insufficient to account for deviations of the magnetic moments from the Schmidt lines. Moreover, the pairing force which we use to approximate the short range force does differ from an actual short range δ-force in several ways. Although these differences do not seem to show up in calculations of the gross properties of the nuclear wave function, it is easy to see that they are extremely important in calculating magnetic moments. If we assume that an improved Hamiltonian, H_R, is of the form of a δ-function force and a $P^{(2)}$ force,

$$H_R = \sum_j{}' \varepsilon_j + \frac{1}{2} \sum_{ij}{}' v(r_i, r_j) \, \delta(r_i - r_j) + \frac{\chi}{2} \sum_{ij}{}' P^{(2)}(ij), \tag{60}$$

then the Hamiltonian, H, used in this work is related to this Hamiltonian by

$$H_R = H + V, \tag{61}$$

where

$$V = \sum_{ij} v\,(r_i, r_j)\,\delta\,(r_i - r_j) - \sum_{ij} G_{ij}, \tag{62}$$

and G_{ij} is the pairing force as defined in Chapter II. If we use V as the perturbation in calculating the extra configuration mixing which plays a part for magnetic moments, then the calculation is quite similar to that of Ref. 30.

As these authors point out, there are only a few kinds of admixed configurations which can change the magnetic moments in first order perturbation theory on shell model states. There are two such kinds of admixtures. First, when the unperturbed state has an even number of particles in both the $j_1 = l_1 + 1/2$ and the $j_2 = l_1 - 1/2$ shells of a spin-orbit doublet, and the upper level is not filled, there are contributing configurations in which one particle in the lower level is elevated to the higher level, with a total angular momentum for particles in the two levels being unity. I.e., the original configuration $j_1^{n_1}(0)\,j_2^{n_2}(0)$ is changed to $\left[j_1^{n_1-1}(j_1)\,j_2^{n_2+1}(j_2)\right](1)$. The second type is quite similar, but in this case a particle is transferred between the states of the particles in the odd group and its spin orbit partner.

Our pairing force does not admix configurations of these types and, since the strength of the pairing force needed in our calculations gives about the same gap as the force used in Ref. 30 for configurations of identical particles, we can use the same δ-force to obtain the admixed configurations instead of using V. As a rough check on the consistency of our wave functions with the experimental values of the magnetic moments, we carry out a configuration mixing calculation with a δ-function force with the same parameters as used in Ref. 30. We use constant radial matrix elements. Our calculation differs from that of Arima and Horie only in that (i) our ground state wave functions are admixtures of many different configurations with mixture coefficients given by our pairing force calculation, the only configurations which are in our odd-A ground state wave functions neglecting the phonon admixtures, being of the type $j_1^{n_1}(0)\,j_2^{n_2}(0)$ $\ldots j^{P-1}(0)\,j; jm\rangle$, where j is the angular momentum of the ground state quasi-particle; and (ii) our wave functions contain a spread in the number of particles.

In Table II we give the results of this calculation. The wave functions used are those parts of the one quasi-particle states which have the correct number of particles. The calculation was carried out for only one Sn isotope since the results will be similar for the other two Sn isotopes in which the

TABLE II

Magnetic moments in odd-A nuclei. $\mu_{s.p.}$ is the Schmidt value for the isotope. The experimental values are taken from Ref. 32.

Isotope	Spin	$\mu_{s.p.}$	$\mu_{theor.}$	μ_{exp}
Ni^{61}	$(3/2)^-$	-1.91	-0.21	0
La^{139}	$(7/2)^+$	1.72	2.24	2.76
Pr^{141}	$(5/2)^+$	4.79	3.92	3.92
Sn^{115}	$(1/2)^+$	-1.91	-0.70	-0.91

magnetic moment is known. In the $N = 28$ region our wave functions with a fixed number of particles are almost pure configurations, so there is almost no change in the results of Ref. 30.

For the most part, our results are an average of the results of configurations used in Ref. 30, although this is not always true. It would take a detailed calculation to prove that the magnetic moments of odd-A nuclei can actually be determined by this method; however, one sees that perturbations of the type considered produce shifts of the magnetic moments from the Schmidt lines of the observed order of magnitude.

VII. Electromagnetic Transition Rates

In addition to the valuable information concerning parity and spins considered in § III, electromagnetic transition rates can yield much more detailed information about the wave functions of nuclear states. We have already seen how the strong enhancement of the $E2$ transition rates in even-A nuclei not only can be used to identify the collective states, but that the magnitude of the transition rates can help select the proper force strengths for our pairing and $P^{(2)}$ type of force (cf. § III. B). In this chapter, we investigate more systematically the electromagnetic transition rates from the collective 2^+ states in the even-A nuclei as well as the single-particle part of the transitions from quasi-particle states.

A. Odd-A Nuclei

Electromagnetic transitions between states in odd-A nuclei will proceed by both particle and collective types of operators. The latter type will be most important for $E2$ transitions. But since there is at present no evidence

on this type of transition, we restrict ourselves to the single-particle part of the transition operator. For any single-particle operator, the matrix element for a transition from a single quasi-particle state of angular momentum j_i to a single quasi-particle state of angular momentum j_f is given by

$$(\Psi_{j_f m_f} | \mathfrak{D} | \Psi_{j_i m_i}) = (U_{j_f} U_{j_i} - (-1)^T V_{j_f} V_{j_i}) \langle j_f m_f | \mathfrak{D} | j_i m_i \rangle, \qquad (63)$$

where $\langle j_f m_f | \mathfrak{D} | j_i m_i \rangle$ is the ordinary single-particle matrix element. In equation (63) the factor $(-1)^T$ is ± 1, depending upon whether the operator is even or odd under time reversal, i.e., $\tau 0 \tau^{-1} = (-1)^T \mathfrak{D}$; or in terms of the matrix elements,

$$\langle \tau j_i m_i | \mathfrak{D} | \tau j_f m_f \rangle = (-1)^T \langle j_f m_f | \mathfrak{D} | j_i m_i \rangle. \qquad (64)$$

The single-particle operators for the electric and magnetic 2^L pole transitions are

$$\mathfrak{M}(EL) = f_1(r) Y_M^L + i f_2(r) \boldsymbol{\sigma} \times \boldsymbol{r} \cdot \operatorname{grad} Y_M^L, \qquad (65\,a)$$

$$\mathfrak{M}(ML) = f_3(r) \boldsymbol{L} \cdot \operatorname{grad} Y_M^L + f_4(r) \boldsymbol{\sigma} \cdot \operatorname{grad} Y_M^L, \qquad (65\,b)$$

where the $f_i(r)$ are real functions of the scalar r. From these we see that

$$\langle \tau j_i m_i | \mathfrak{M}(EL) | \tau j_f m_f \rangle = \langle j_f m_f | \mathfrak{M}(EL) | j_i m_i \rangle, \qquad (66\,a)$$

$$\langle \tau j_i m_i | \mathfrak{M}(ML) | \tau j_f m_f \rangle = -\langle j_f m_f | \mathfrak{M}(ML) | j_i m_i \rangle, \qquad (66\,b)$$

holds for all values of L. Therefore, from equation (63)

$$(\Psi_{j_f m_f} | \mathfrak{M}(EL) | \Psi_{j_i m_i}) = (U_{j_f} U_{j_i} - V_{j_f} V_{j_i}) \langle j_f m_f | \mathfrak{M}(EL) | j_i m_i \rangle \quad (67\,a)$$

$$(\Psi_{j_f m_f} | \mathfrak{M}(ML) | \Psi_{j_i m_i}) = (U_{j_f} U_{j_i} + V_{j_f} V_{j_i}) \langle j_f m_f | \mathfrak{M}(ML) | j_i m_i \rangle. \quad (67\,b)$$

From equations (67a) and (67b) one can express the lifetimes for transitions between one quasi-particle states in terms of the lifetime for transitions between single-particle states with the same electrical properties, angular momenta, and energy separation. Calling the lifetime of the single-particle states $\tau^{\text{s. p. } 33)}$, the reciprocal lifetimes for the single quasi-particle transitions are

$$\frac{1}{\tau_{i \to f}} = D_{fi} \frac{1}{\tau_{i \to f}^{\text{s. p.}}}, \qquad (68)$$

with

$$D_{fi}(ML) = \frac{1}{2}\left[1 + \frac{(\varepsilon_f - \lambda)(\varepsilon_i - \lambda)}{\sqrt{(\varepsilon_f - \lambda)^2 + \Delta^2}\sqrt{(\varepsilon_i - \lambda)^2 + \Delta^2}}\right.$$

$$\left. + \sqrt{\left(1 - \frac{(\varepsilon_f - \lambda)^2}{(\varepsilon_f - \lambda)^2 + \Delta^2}\right)\left(1 - \frac{(\varepsilon_i - \lambda)^2}{(\varepsilon_i - \lambda)^2 + \Delta^2}\right)}\right] \qquad (69\,\mathrm{a})$$

$$D_{fi}(EL) = \frac{1}{2}\left[1 + \frac{(\varepsilon_f - \lambda)(\varepsilon_i - \lambda)}{\sqrt{(\varepsilon_f - \lambda)^2 + \Delta^2}\sqrt{(\varepsilon_i - \lambda)^2 + \Delta^2}}\right.$$

$$\left. - \sqrt{\left(1 - \frac{(\varepsilon_f - \lambda)^2}{(\varepsilon_f - \lambda)^2 + \Delta^2}\right)\left(1 - \frac{(\varepsilon_i - \lambda)^2}{(\varepsilon_i - \lambda)^2 + \Delta^2}\right)}\right], \qquad (69\,\mathrm{b})$$

where $D(ML)$ and $D(EL)$ are the reduction factors for magnetic and electric 2^L pole transitions, respectively. From equation (69) one can easily see the effect of the pairing force upon the transition rates. If the states i and f are both far above the position of the chemical potential, so that $\frac{\varepsilon - \lambda}{\sqrt{(\varepsilon - \lambda)^2 + \Delta^2}} \simeq 1$, the transition rate is single-particle. This is the case when the probablility of the ground state containing a configuration with particles in these states is almost zero. As one adds particles, λ approaches the value ε_f, from below, and both the electric and magnetic reduction factors diminish in size, but the reduction of the electric transitions below the single-particle value is faster than the reduction in the magnetic transitions. For example, when $\varepsilon_i - \varepsilon_f \ll \Delta$, by the time $\lambda = \varepsilon_f$, equation (69) shows $D(ML) = 1$ while $D(EL) = 0$. This is quite a different behaviour than would be predicted by a pure shell model or a shell model with a diagonal pairing energy. (By a diagonal pairing force we mean a pairing force which acts within each j-shell with no matrix elements between different j-shells). For instance, in the magnetic case, the non-diagonal matrix elements of the pairing force are very important in keeping the matrix element approximately constant while the chemical potential, λ, moves through two close lying levels. This feature depends simply on populating both of these states equally. Since one does not do this in either a non-interacting shell model or with a diagonal pairing force, the magnitude of the reduction factor will vary much more in these cases as the number of particles is changed. Generally, the result is that the magnetic transitions tend to vary rather more gradually with changes in the number of particles than the shell model result, and that the electric transitions can display strong reductions even in pure quasi-particle states. In comparing the experimental transition rates to the theoretical ones it is most significant to compare the experimental with
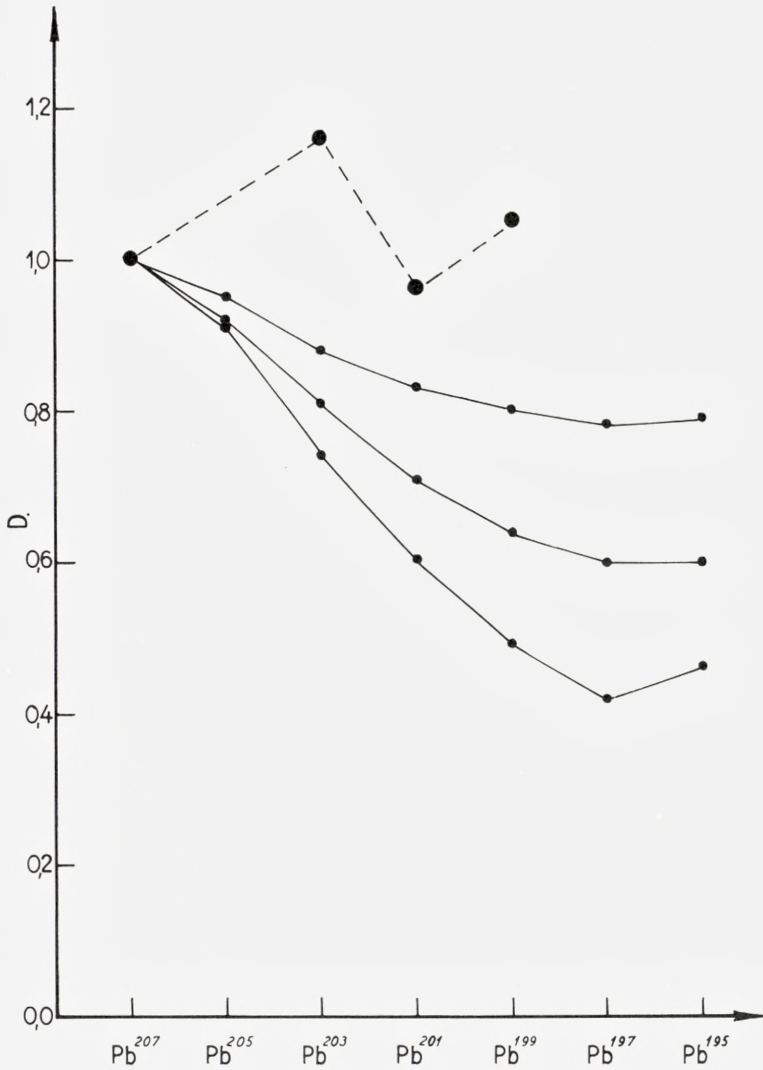
Fig. 26. $M4$ *transition rate in odd-A Pb isotopes.*

Curves a, b, c are the theoretical values of the reduction from single-particle for $G = 30/A$, $23/A$, and $19/A$. The experimental values[19] are normalized at Pb^{222}.

the theoretical reduction factors in order to remove the very large effects of energy differences.

In the odd-A s.c.s. nuclei, the only lifetimes which have been measured are those of the isomeric states. The most complete results are for the Pb

isotopes, for which the $M4$ transitions between the $i_{13/2}$ and $f_{5/2}$ states have served so well to trace the position of the $i_{13/2}$ state (cf. Chapter III). The lifetimes are measured in Pb^{207}, Pb^{203}, Pb^{201}, Pb^{199}, and Pb^{197} [19]. The comparison of the experimental reduction factors with the prediction of the pairing force calculation is made in Fig. 26. The single-particle 2^L pole electromagnetic transition rate has an energy dependence given by $(E_i - E_f)^{2L+1}$. Using this dependence and the experimental lifetimes, energies, and conversion coefficients, one finds that the experimental reduction is almost constant for the five isotopes. These "experimental" reduction factors are based on a comparison with a single-particle estimate which neglects shell effects on the nuclear radii, an approximation which could affect the relative $M4$ reduction factors, where the nuclear radius enters in the sixth power.

The values plotted in the figure are normalized to the Pb^{207} value, which is unity in our model. Because of the uncertainty in the experimental reduction factor, a detailed comparison with the theoretical curves may not be significant. It is of interest, however, that, for the values of G indicated by other evidence, the $M4$ reduction factors are indeed expected to vary only little over the isotopes considered. As already mentioned, this would

TABLE III

Electromagnetic transitions in one quasi-particle states. $D_{exp} = P_{exp}/P_{s.p.}$, where $P_{s.p.}$ is a theoretical estimate of the transition when treated as single-particle.[33] D_{theor} is for $G = 0.128$ in Pb, 0.187 in Sn, and 0.238 in $N = 50$. a_0 is the radius parameter.

Element	Transition	Assumed Level Change	D_{exp} ($a_0 = 1.2$)	D_{exp} ($a_0 = 1.1$)	$D_{theor.}$
Pb^{207}	1.064 M4	$i_{13/2} \to f_{5/2}$	0.25	0.42	1.00
Pb^{205}		$i_{13/2} \to f_{5/2}$			0.93
Pb^{203}	0.825 M4	$i_{13/2} \to f_{5/2}$	0.30	0.49	0.85
Pb^{201}	0.629 M4	$i_{13/2} \to f_{5/2}$	0.24	0.41	0.78
Pb^{199}	0.424 M4	$i_{13/2} \to f_{5/2}$	0.26	0.44	0.73
Pb^{197}	0.235 M4	$i_{13/2} \to f_{5/2}$	0.27	0.46	0.70
Pb^{195}		$i_{13/2} \to f_{5/2}$			0.70
Sn^{117}	0.159 M4	$h_{11/2} \to d_{3/2}$	0.41	0.68	0.96
Sn^{119}	0.065 M4	$h_{11/2} \to d_{3/2}$	0.57	0.95	0.94
$_{39}Y^{89}_{50}$	0.913 M4	$g_{9/2} \to p_{1/2}$	0.26	0.43	0.68
$_{41}Nb^{91}_{50}$	0.105 M4	$g_{9/2} \to p_{1/2}$	0.20	0.33	0.48
$_{43}Tc^{93}_{50}$	0.390 M4	$p_{1/2} \to g_{9/2}$	0.35	0.59	0.65

not have been the case if the configuration mixing introduced by the pairing force had not been taken into account. As to the absolute values of the transition probabilities, the single-particle estimate for the expected nuclear radius is larger by a factor of two or three than the experimental value for Pb^{207}; however, there is considerable uncertainty in the theoretical single-particle estimate (cf. Table III, p. 67).

The lifetimes of the $h_{11/2}$ states are known in Sn^{117} and Sn^{119} [34]. The internal conversion coefficients, which are quite large for these transitions, have not been measured. However, the errors in the values of D_{exp}, the experimental reduction factor introduced by using the theoretical values of the internal conversion coefficients[35], are less than those due to the uncertainty in the single-particle estimate. The theoretical value of the $M4$ reduction factor in the pairing force calculation is almost unity, since in this case the separation between the $d_{3/2}$ and $h_{11/2}$ levels is small compared to the gap. These results would be approximately unaltered for any values of the pairing strength and of the single-particle energies which fit the spins and energy levels, as well as the $2^+ \rightarrow 0^+$ transition rates of the Sn isotopes. Table III, in which D_{theor}, the value of the reduction factor in the pairing calculation, is calculated with a pairing strength and single-particle energy levels used to give the results shown in Fig. 6, indicates that the experimental and theoretical results are consistent.

In the $N = 50$ region, lifetimes have been measured for three $M4$ transitions between the $p_{1/2}$ and $g_{9/2}$ states: $_{39}Y^{89}$, $_{41}Nb^{91}$, and $_{43}Tc^{93}$ [21]. Using the theroretical conversion coefficients, one finds that the reduction factors given by the experiments and the single-particle estimates are consistent with the pairing force results. The values of D_{theor} quoted in the table are calculated from the energy levels and pairing strength which leads to the energy levels of Fig 13. The heightened reduction in the $M4$ matrix elements for $_{41}Nb^{91}_{50}$ apparently reflects the diminution in the gap due to the filling of the level with spin $1/2$, which is far in energy from other levels, as discussed in § III. The relative values of the experimental reduction factors also show a dip for Nb^{91} compared to Y^{89} and Tc^{93}, although this might not be accurate enough to be significant.

In the $N = 82$ region the lifetimes are known for the 0.165 Mev $M1$ transition in La^{139} and the 0.142 Mev $M1$ transition in Pr^{141}. However, both of these transitions are "l-forbidden", and a configuration mixing calculation of the same kind as was used for magnetic moments (§ V) would therefore be needed in order to account for these transitions[36]. The 0.024 Mev transition in Sn^{119} is also l-forbidden.

In a similar way, perturbations must also admix other configurations to all the single quasi-particle states. The amount of admixture would presumably depend upon the unperturbed states, and thus would vary for a one quasi-particle state of a particular type as the number of particles changes. Such effects could alter some of the quantitative results, for instance, in the $M4$ reduction factors.

B. Even-A Nuclei

1. *Single-Particle Transitions in Two Quasi-Particle States*

In the same way as the result (68) was obtained for one quasi-particle states, for a transition between two states which can be described as two quasi-particle states, $\Psi_i [j_1 j_i]^J \rightarrow \Psi_f [j_1 j_f]^{J'}$, the reciprocal lifetime is given by

$$\frac{1}{\tau_{i \rightarrow f}} = D_{if} \frac{1}{\tau_{i \rightarrow f}^{\text{s.p.}}}, \tag{70}$$

where $\tau^{\text{s.p.}}$ is the single-particle lifetime* for the electromagnetic $(2)^L$ multipole transition $J \rightarrow J'$, $j_i \rightarrow j_f$.

The best experimental comparison can be made for transitions from the high angular momentum odd-parity states discussed in § III. These states may often represent rather unique quasi-particle configurations. We restrict our discussion to those cases in which the experimental lifetimes are known.

The 7^- to 6^+ $E1$ transition in Sn^{170} is reduced about 2.5×10^{-8} compared to a single-particle estimate. Since there are no possible shell model configurations in this region of isotopes which would lead to $E1$ transitions, any shell model theory would lead to a transition rate of essentially zero.

The half-life of the 2.2 Mev state in Pb^{206} is 1.25×10^{-4} sec.[22), 37)]. We predict that this 7^- state is mainly a combination of an $i_{13/2}$ quasi-particle coupled with a $p_{3/2}$ quasi-particle and an $f_{5/2}$ quasi-particle. The 2.00 and 1.68 Mev 4^+ states to which the 7^- states decay by $E3$ transitions are mainly combinations of the $(f_{5/2} p_{3/2})_4$ and $(f_{5/2})_4^2$ two quasi-particle states. For these main parts of the wave functions the $E3$ single-

---

* $\tau_{i \rightarrow f}^{\text{s.p.}}$ in Eq. (70) is related to Moszkowski's $\tau_{i \rightarrow f}^{\text{s.p.}}$ in Ref. 33 by

$$\frac{1}{\tau_{i \rightarrow f}^{\text{s.p.}}} = (2J' + 1)(2j_i + 1) \, | \, W \, (j_f J' j_i J; j_1 L) |^2 \left(\frac{1}{\tau_{i \rightarrow f}^{\text{s.p.}}} \right)$$

Moszkowski.

particle transition is forbidden. There will also be a certain amount of the $(f_{5/2} f_{7/2})_4$ and $(p_{3/2} f_{7/2})_4$ two quasi-particle states in these 4^+ states, which allow the $E3$ transitions; however, we expect the transition rate to be far below single-particle. In units of the single-particle estimate, the transition
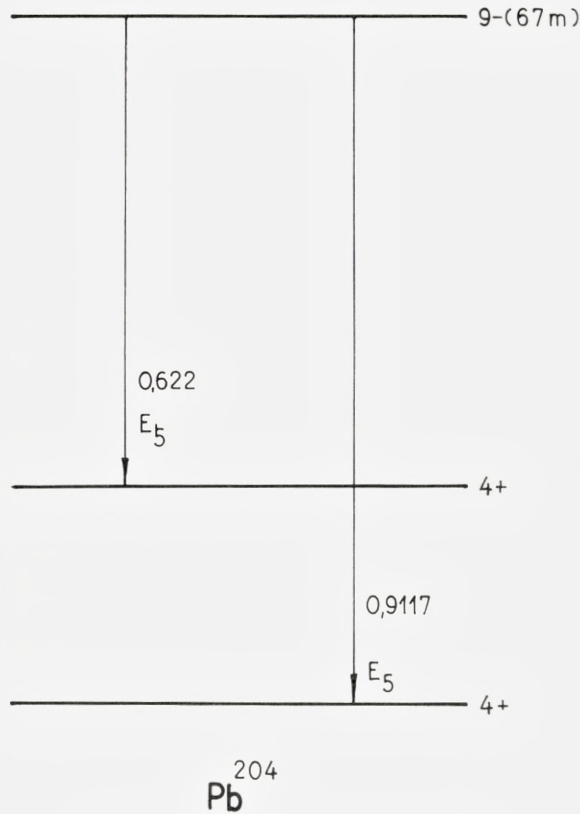
Fig. 27. *Decay of the 9^- state in Pb²⁰⁴.*

strengths for the 0.202 and 0.516 Mev transitions are of the order of 0.3, which seems to be somewhat large from the considerations mentioned above. However, it is difficult to estimate the amount of mixing of quasi-particle configurations which does occur.

The half-life of the 9^- state in Pb²⁰⁴ is measured to be 4.02×10^3 sec[38] for decay into two 4^+ states by a 0.912 and a 0.622 Mev $E5$ transition. The 9^- state is mostly a state of an $i_{13/2}$ and an $f_{5/2}$ quasi-particle coupled

to their maximum spin. We find that the 4^+ final state for the 0.912 Mev transition is mainly a state of two $f_{5/2}$ quasi-particles, while the 4^+ state associated with the 0.662 Mev transition is mainly one with one $f_{5/2}$ and one $p_{3/2}$ quasi-particle. Of course, these states are so close in energy that
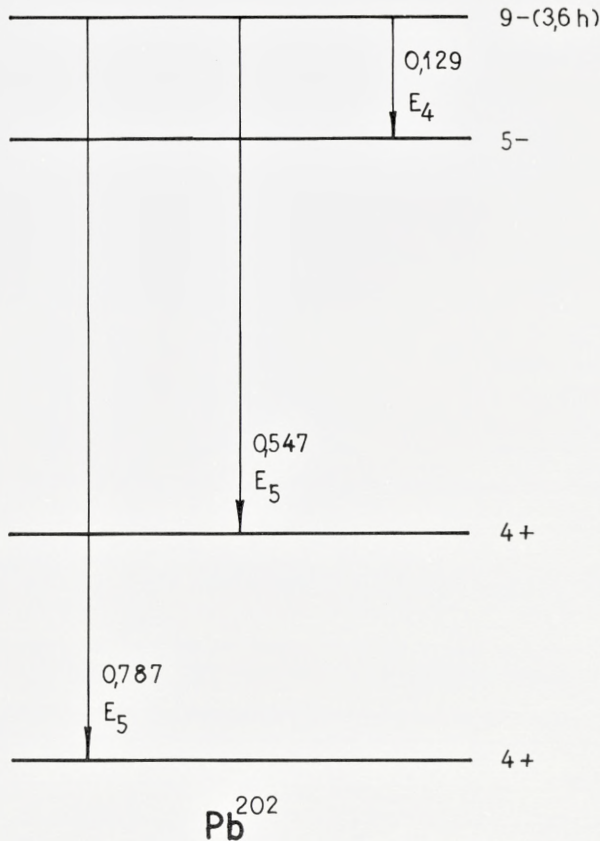
Fig. 28. *Decay of the 9^- state in Pb^{202}.*

one can expect an admixture of these configurations. Table IV shows that the 0.622 Mev transition is consistent with a description that it proceeds via a two quasi-particle transition between the states which are expected to dominate, the reduction factor being about 0.7. The 0.912 Mev transition, however, is enhanced compared to the theoretical value by a factor of the order of 100 if the transition proceeds via $(i_{13/2} f_{5/2})_9 - \rightarrow (f_{5/2})_4^2 +$.

<div align="center">TABLE IV</div>

Electromagnetic transitions in two quasi-particle states. $G = 0.128$ (in Pb). The column titled "Assumed Level Change" indicates the type of the quasi-particle which changes during the transition. Where two assumptions have been made for the spin assignments, the states might be admixtures, with the first assignment having the heaviest weight. $D_{\exp}$ is given in units of $(e_{\mathrm{eff}}/e)^2$.

Element	Transition	Assumed Level Change	$D_{\exp}$ $(a_0 = 1.2)$	$D_{\exp}$ $(a_0 = 1.1)$	D_{theor}
Pb^{206} ...	0.516 E3	$[i_{13/2}p_{3/2}]_{7-} + [i_{13/2}f_{5/2}]_{7-}$ $\rightarrow [f_{7/2}p_{3/2}]_{4+} + [f_{7/2}f_{5/2}]_{4+}$	0.26	0.45	0.98 × prob. of $f_{7/2}$ quasi-particle in 4^+ state
	0.202 E3	$[i_{13/2}p_{3/2}]_{7-} + [i_{13/2}f_{5/2}]_{7-}$ $\rightarrow f_{7/2}p_{3/2}]_{4+} + [f_{7/2}f_{5/2}]_{4+}$	0.18	0.29	
Pb^{204} ...	0.912 E5	$[f_{5/2}i_{13/2}]_{9-} \rightarrow [f_{5/2}p_{3/2}]_{4+}$	47	112	0.58
		$[f_{5/2}i_{13/2}]_{9-} \rightarrow [f_{5/2}p_{3/2}]_{4+}$	2.6	6.2	0.73
	0.622 E5	$[f_{5/2}i_{13/2}]_{9-} \rightarrow [f_{5/2}p_{3/2}]_{4+}$	0.4	0.94	0.73
		$[f_{5/2}i_{13/2}]_{9-} \rightarrow [f_{5/2}]^2_{4+}$	7	17	0.58
Pb^{202} ...	0.787 E5	$[f_{5/2}i_{13/2}]_{9-} \rightarrow [f_{5/2}]^2_{4+}$	37	88	0.56
		$[f_{5/2}i_{13/2}]_{9-} \rightarrow [f_{5/2}p_{3/2}]_{4+}$	2.1	4.9	0.34
	0.547 E5	$[f_{5/2}i_{13/2}]_{9-} \rightarrow [f_{5/2}p_{3/2}]_{4+}$	0.31	0.74	0.34
		$[f_{5/2}i_{13/2}]_{9-} \rightarrow [f_{5/2}]^2_{4+}$	5.6	13	0.56
	0.129 E4	$[i_{13/2}f_{5/2}]_{9-} \rightarrow [i_{13/2}p_{3/2}]_{4-}$	0.29	0.60	0.15
Sn^{120} ...	0.089 E1		2.5×10^{-8}		0

Even if the 4^+ state is taken as a $(f_{5/2}p_{3/2})_4$ two quasi-particle state, this $E5$ transition is enhanced by a factor of perhaps 5.

    In Pb^{202} there is a situation which is almost identical to the one in Pb^{204} (cf. Fig. 28)[39), 40)]: a 0.787 Mev $E5$ transition which might be expected from energy considerations to be largely between $(i_{13/2}f_{5/2})_9$ and $(f_{5/2})^2_4$ two quasi-particle states, and a 0.547 Mev $E5$ transition which might be expected to be largely $(i_{13/2}f_{5/2})_{9-} \rightarrow (f_{5/2}p_{3/2})_{4+}$, corresponding to the 0.912 Mev and 0.622 Mev transitions in Pb^{204}, respectively.

    For the 0.547 Mev transition, a reduction factor of 0.34, which results from the pairing force calculation with the assumption of a $(i_{13/2}f_{5/2})_{9-} \rightarrow (f_{5/2}p_{3/2})_{4+}$ transition, is consistent with the experimental results. However,

the 0.787 Mev transition seems to be strongly enhanced above the theoretical value, resembling the 0.912 Mev transition in Pb^{204}.

The 9^- state in Pb^{202} decays with a $37^0/_0$ probability into a 5^- state by a 0.129 Mev $E4$ transition.[39] As explained in § III, the 5^- state associated with the $(i_{13/2} f_{5/2})$ two quasi-particle states is placed above the 9^- state by a $P^{(2)}$ force in perturbation theory, while the 5^- state lies lowest in the $(i_{13/2} p_{3/2})$ two quasi-particle configuration. Moreover, these results are in agreement with the detailed calculations in Pb^{206}.[41] We thus expect the 0.129 Mev $E4$ transition in Pb^{202} to correspond to a transition between the $(i_{13/2} f_{5/2})_{9-}$ and $(i_{13/2} p_{3/2})_{5-}$ two quasi-particle states. Table IV shows that a theoretical reduction factor of 0.15 is consistent with the experimental results if we use this interpretation.

2. The $2^+ \to 0^+$ $E2$ Transitions

As indicated in the discussion of the choice of parameters, the $B(E2)$ values for the lowest $2^+ \to 0^+$ transition of the collective state may be used to determine the effective charge.[42] In Table V we list the experimental $B(E2)$ values together with the theoretical values for the s.c.s. nuclei for which the 2^+ level has been seen. The theoretical values are calculated using (34) with $e_{\text{eff}} = 1$ for the closed proton shell nuclei and $e_{\text{eff}} = 2$ for the closed neutron shell nuclei.

It is seen that the correct value of the $B(E2)$ is obtained for Pb^{206} with use of the experimentally measured effective charge $e_{\text{eff}} = 1.1$[13]. The Sn $B(E2)$ values are also reasonably well accounted for by $e_{\text{eff}} = 1$. For the Ni isotopes a somewhat larger value of e_{eff} seems to be required——about $e_{\text{eff}} = 1.4$. All of the closed neutron shell nuclei seem to require an effective charge well above unity to fit the few measured values, as expected. However, the value $e_{\text{eff}} = 2$ seems to be a little too high. A value $e_{\text{eff}} = 1.5$ would give a better fit to the $B(E2)$ of these nuclei.

In conclusion, the experimental values for the reduction in the $M4$ transition rates in the odd-A Pb isotopes appear to be rather constant, which is consistent with the theoretical reductions for the values of G used in this work. The theoretical reduction factors for $M4$ transitions in the other odd-A s.c.s. nuclei are also consistent with experiment, in all cases the reduction factor being not less than 0.5 (and greater than 0.7, except in rather unusual cases). This result can be extended qualitatively to other nuclei. In every case, the pairing correlations will tend for magnetic transitions to maintain the transition rate near the single-particle value even as particles

TABLE V. $B(E2)$ *values*

The theoretical and experimental $B(E2)$ $0^+ \to 2^+$ reduced transition probability is shown for s.c.s. nuclei. The value $e_{eff} = 1$ is used in computing the theoretical value for Pb, Sn, and Ni, and $e_{eff} = 2$ for $N = 82$, $N = 50$, and $N = 28$. In the fourth column the "single-particle" estimate $B(E2)_{s.p.}$ $= 3 \cdot 10^{-5} A^{4/3} e^2 \cdot 10^{-48} \, cm^4$ was used; and in the last column the experimental references are given.

Isotope	$B(E2)_{exp}$ $e^2 \, 10^{-48} \, cm^4$ Theoretical	$B(E2)_{exp}$ $e^2 \, 10^{-48} \, cm^4$ Experimental	$\dfrac{B(E2)_{exp}}{B(E2)_{s.p.}}$	Ref.
Pb^{206}	0.13	0.14	4	(22)
Pb^{204}	0.22			
Pb^{202}	0.29			
Pb^{200}	0.33			
Sn^{112}	0.25	0.18	11	(44)
Sn^{114}	0.20	0.20	11	(44)
Sn^{116}	0.26	0.21	12	(22)
Sn^{118}	0.29	0.23	13	(22)
Sn^{120}	0.28	0.22	13	(22)
Sn^{122}	0.25	0.25	14	(22)
Sn^{124}	0.20	0.21	12	(22)
Ni^{58}	0.020	0.072	11	(45)
Ni^{60}	0.046	0.091	13	(45)
Ni^{62}	0.071	0.083	11	(45)
Ni^{64}	0.068			
Xe^{136}	0.34			
Ba^{138}	0.51			
Ce^{140}	0.73	0.36	16	(46)
Nd^{142}	1.01			
Sr^{88}	0.180	0.13	12	(46)
Zr^{90}	0.113			
Ti^{50}	0.078			
Cr^{52}	0.16	0.085	14	(46)
Fe^{54}	0.23			

are placed in the levels involved in the transition——a result which might explain the striking constancy in the $M4$ reduction factors throughout the periodic table.[43]

For even-A nuclei, we conclude that our results for quasi-particle transition rates are consistent with experiment within the accuracy obtainable by our methods, with the possible exception of an enhancement of

certain $E5$ transitions in Pb^{204} and Pb^{202}. For the collective states, the lifetimes can be used to determine the effective charge. In addition, in Pb^{206} we can use the experimentally measured value of e_{eff} to help select G.

As the systematic experimental data is extended, the transition rates will provide a detailed test of the wave functions obtained with this model.

VIII. Summary

An approximate calculation of the properties of nuclei with one closed proton or neutron shell is attempted. Using the approximation methods introduced by the theory of superconductivity, we have calculated the effects of those parts of the short range part of the residual interaction which are common to the pairing force, obtaining the quasi-particle energies for several strengths, G, of the pairing force. The deformed field approximation is used to calculate the effect of the relatively long range part of the nuclear force, and in particular to determine the positions and B($E2$)'s of the 2^+ collective states in the even-A isotopes.

The most important systematic experimental feature for the even-A s.c.s. isotopes is the position of the first excited 2^+ state. This state, which is of collective character, has a rather constant energy above the ground state, and is often quite a bit lower in energy than the next higher excited states, thus lying in the gap between the ground state and the intrinsic excited states.

We find a simple explanation for this 2^+ state. This state, which in our work is always the first excited quadrupole vibrational level, is located below the first states of two quasi-particles, sometimes rather far below, as in the case of the Sn isotopes. In every case, the second excited vibrational level is among the quasi-particle states so that it becomes more difficult to explore the possibility of higher collective states.

Also in even-A nuclei we find that we can approximately derive not only the positions of the 2^+ levels, but also the positions of the levels of high angular momentum with values of the pairing and $P^{(2)}$ force which do not differ much from region to region, except for the A dependence of a volume force.

For the odd-A isotopes, the most significant systematic experimental feature is the gradual change in the positions of the states which correspond

to our one quasi-particle states, motions which are much smoother than those predicted by an independent shell model.

In the odd-A isotopes the positions of the quasi-particle levels do not depend upon the strengths of the pairing and $P^{(2)}$ force so much as upon the separation of the single-particle energy levels, for values of the pairing force which are consistent with the data in the even-A isotopes. The ground state spins are determined within the accuracy expected. In Pb, where both the single-particle well is known and systematic measurements for the position of the $i_{13/2}$ states have been made, we find that we can quite accurately and rather unambiguously predict the relative position of the $i_{13/2}$ state.

The even-odd mass data gives values for the gap which are in agreement with our results. The determination of the absolute binding energy involves questions which are beyond the scope of our methods, but the experimental data seems to be consistent with our results.

Very little data is available on quadrupole moments of s.c.s. nuclei, but our calculated values are in fair agreement with experiment when one considers the change which can occur with the inclusion of small admixtures of configurations other than those arising from a pairing plus $P^{(2)}$ interaction. The magnetic moment data is much more extensive. Although for our wave functions the calculated magnetic moments are too close to the single-particle values, the small admixture of other configurations can change these moments by amounts of the right order to agree with experiment.

The main systematic results from the theoretical study of the collective part of the electromagnetic transition rate is the theoretical value for the effective charge. The main systematic feature which we have calculated for electromagnetic transitions between quasi-particle states is the tendency for the $M4$ reduction factors to remain rather constant for the $i_{13/2} \rightarrow f_{5/2}$ $M4$ transitions in the Pb odd-A isotopes, which seems to be indicated by the experiments. This feature depends essentially on the strongly mixed configurations which occur in our calculation. Qualitatively, this result would tend to lead to a rather constant reduction factor for magnetic transitions compared to electric transitions, which is a possible explanation for the striking constancy in the $M4$ reduction factors, while the $E3$ reduction factors are widely varying.

We conclude that the simple model which we have tried has been successful in deriving the observed low energy systematic features of s.c.s. nuclei, and that our results might serve as a good basis for a more detailed quantitative investigation.

Acknowledgements

Appendix

In this Appendix we list the quantities needed to obtain the nuclear energy levels and wave functions for typical strengths of the pairing force parameter, G, and long range force parameter, X, which are consistent with the known energy levels. For each region, the single-particle energies, ε_j, are given, with the subscript giving the angular momentum of the level. Using Eqs. (9) and (10), the quasi-particle energies are determined for each isotope by λ and Δ, which is listed in the table.

The properties of the collective state are conveniently calculated from the quantities $\mathfrak{A}$ and $\mathfrak{B}$, which are included in the table for each isotope, defined by

$$\mathfrak{A} = \sum_{jj'}{}' \frac{(U_j V_{j'} + V_j U_{j'})^2}{E_j + E_{j'}} \frac{1}{10} (2j'+1) \left(C^{2\ j'\ j}_{0\ \frac{1}{2}\ \frac{1}{2}} \right)^2 \frac{\langle j \,|\, r^2 \,|\, j' \rangle^2}{\langle j \,|\, r^2 \,|\, j \rangle_u^2}, \qquad \text{A(1)}$$

$$\mathfrak{B} = \sum_{jj'}{}' \frac{(U_j V_{j'} + V_j U_{j'})^2}{(E_j + E_{j'})^3} \frac{1}{10} (2j'+1) \left(C^{2\ j'\ j}_{0\ \frac{1}{2}\ \frac{1}{2}} \right)^2 \frac{\langle j \,|\, r^2 \,|\, j' \rangle^2}{\langle j \,|\, r^2 \,|\, j \rangle_u^2}, \qquad \text{A(2)}$$

where $\langle j \,|\, r^2 \,|\, j \rangle_u^2$ is defined in Eq. (41). The relation of these quantities to the collective parameters B and C of Eq. (3) is given by

$$B = \frac{1}{2} \frac{\beta}{\alpha^2} \frac{1}{\frac{5}{4\pi} \langle \,|\, r^2 \,|\, \rangle_u^2} \qquad \text{A(3)}$$

$$C = \frac{1}{2\alpha} [1 - 2\alpha X] \frac{1}{\frac{5}{4\pi} \langle \,|\, r^2 \,|\, \rangle_u^2} \qquad \text{A(4)}$$

$Z = 82$, holes in the $N = 126$ shell (Pb isotopes) for $G = 0.111$ Mev.

$\varepsilon_{p_{1/2}} = 0$, $\varepsilon_{f_{5/2}} = 0.57$, $\varepsilon_{p_{3/2}} = 0.90$, $\varepsilon_{i_{13/2}} = 1.634$, $\varepsilon_{f_{7/2}} = 2.35$ Mev.

A	λ (Mev)	Δ (Mev)	$\mathfrak{A}$ (Mev^{-1})	$\mathfrak{B}$ (Mev^{-3})
206.................	0.11	0.25	0.40	0.50
205.................	0.25	0.34		
204.................	0.33	0.42	0.52	0.42
203.................	0.42	0.48		
202.................	0.52	0.53	0.56	0.33
201.................	0.60	0.55		
200.................	0.69	0.58	0.57	0.27
199.................	0.78	0.60		
198.................	0.88	0.63	0.56	0.20
197.................	0.97	0.64		

$Z = 50$, neutrons in 50—126 shell (Sn isotopes) for $G = 0.187$ Mev.

$\varepsilon_{d_{5/2}} = 0$, $\varepsilon_{g_{7/2}} = 0.22$, $\varepsilon_{s_{1/2}} = 1.90$, $\varepsilon_{d_{3/2}} = 2.20$, $\varepsilon_{h_{11/2}} = 2.80$ Mev.

A	λ (Mev)	Δ (Mev)	$\mathfrak{A}$ (Mev^{-1})	$\mathfrak{B}$ (Mev^{-3})
108	0.17	0.97	0.33	0.061
109	0.29	0.98		
110	0.44	0.98	0.34	0.057
111	0.60	0.97		
112	0.76	0.94	0.33	0.049
113	0.97	0.90		
114	1.20	0.89	0.32	0.044
115	1.43	0.92		
116	1.64	0.96	0.34	0.048
117	1.81	1.00		
118	1.97	1.03	0.35	0.052
119	2.12	1.05		
120	2.26	1.07	0.35	0.054
121	2.40	1.08		
122	2.53	1.07	0.34	0.057
123	2.65	1.06		
124	2.78	1.03	0.32	0.060
125	2.88	1.00		
126	3.01	0.96	0.29	0.060
127	3.12	0.90		
128	3.24	0.83	0.22	0.053
129	3.36	0.72		

$Z = 28$, neutrons in 28—50 shell (Ni isotopes) for $G = 0.331$ Mev.

$\varepsilon_{p_{3/2}} = 0$, $\varepsilon_{f_{5/2}} = 0.78$, $\varepsilon_{p_{1/2}} = 1.56$, $\varepsilon_{g_{9/2}} = 4.52$ Mev.

A	λ (Mev)	Δ (Mev)	$\mathfrak{A}$ (Mev^{-1})	$\mathfrak{B}$ (Mev^{-3})
58	-0.31	0.80	0.11	0.024
59	-0.09	0.94		
60	0.14	1.04	0.18	0.028
61	0.38	1.11		
62	0.59	1.15	0.21	0.032
63	0.84	1.16		
64	1.09	1.14	0.21	0.032
65	1.39	1.08		
66	1.64	0.99	0.15	0.022
67	1.99	0.81		

$N = 82$, protons in 50—82 shell for $G = 0.173$ Mev.

$$\varepsilon_{g_{7/2}} = 0, \ \varepsilon_{d_{5/2}} = 1.0, \ \varepsilon = 2.0 \text{ Mev.}$$

A	λ (Mev)	Δ (Mev)	$\mathfrak{A}$ (Mev^{-1})	$\mathfrak{B}$ (Mev^{-3})
134.................	−0.41	0.54	0.13	0.053
135.................	−0.29	0.65		
136.................	−0.17	0.73	0.22	0.065
137.................	−0.05	0.78		
138.................	0.09	0.83	0.26	0.058
139.................	0.22	0.88		
140.................	0.37	0.92	0.30	0.048
141.................	0.52	0.96		
142.................	0.66	0.99	0.34	0.051
143.................	0.78	1.02		
144.................	0.93	1.06	0.38	0.055
145.................	1.05	1.09		
146.................	1.15	1.11	0.41	0.057

$N = 50$, protons in 28—50 shell for $G = 0.291$ Mev.

$$\varepsilon_{f_{5/2}} = 0, \ \varepsilon_{p_{3/2}} = 0.6, \ \varepsilon_{p_{1/2}} = 1.8, \ \varepsilon_{g_{9/2}} = 3.4 \text{ Mev.}$$

A	λ (Mev)	Δ (Mev)	$\mathfrak{A}$ (Mev^{-1})	$\mathfrak{B}$ (Mev^{-3})
83.................	0.16	0.98		
84.................	0.36	1.01	0.21	0.038
85.................	0.58	1.01		
86.................	0.82	0.98	0.22	0.037
87.................	1.10	0.92		
88.................	1.44	0.86	0.18	0.030
89.................	1.83	0.83		
90.................	2.24	0.84	0.10	0.011
91.................	2.59	0.93		
92.................	2.85	1.00	0.15	0.025
93.................	3.08	1.04		

$N = 28$, protons in 20—28 shell for $G = 0.385$ Mev.

$$\varepsilon_{d_{3/2}} = 0, \ \varepsilon_{f_{7/2}} = 2.5, \ \varepsilon_{p_{3/2}} = 5.57, \ \varepsilon_{f_{5/2}} = 6.54 \text{ Mev.}$$

A	λ (Mev)	Δ (Mev)	$\mathfrak{A}$ (Mev^{-1})	$\mathfrak{B}$ (Mev^{-3})
50.................	1.90	1.12	0.088	0.010
51.................	2.19	1.22		
52.................	2.48	1.26	0.13	0.014
53.................	2.77	1.25		
54.................	3.08	1.18	0.14	0.013
55.................	3.45	1.02	0.13	0.011

References

1. M. G. Mayer, Phys. Rev. **75**, 1969 (1949); **78**, 16 (1950).
   Haxel, Jensen and Suess, Phys. Rev. **75**, 1766 (1949); Z. Physik **128**, 295 (1950).
2. A. Bohr, Mat. Fys. Medd. Dan. Vid. Selsk. **26**, no. 14 (1952).
   A. Bohr and B. R. Mottelson, Mat. Fys. Medd. Dan. Vid. Selsk. **27**, no. 16 (1953).
3. See J. P. Elliott and A. M. Lane, "Handbuch der Physik" XXXIX (Springer: Berlin, 1957), p. 241, for a discussion and references.
4. See F. Villars, Annual Review of Nuclear Science, I, 185 (1957) for a discussion of the work on the derivation of the collective motions and individual references.
5. J. P. Elliott, Proc. Roy. Soc. **245** (A), 128 (1958); 562 (1958).
6. B. Bayman, Proceedings of the International Congress on Nuclear Physics, Paris (1958).
7. Bardeen, Cooper, and Schrieffer, Phys. Rev. **108**, 1175 (1957).
   N. N. Bogolubov, JETP, USSR **34**, 58; 73 (1958).
   — Nuovo Cimento **7**, 794 (1958).
   J. G. Valatin, Nuovo Cimento **7**, 843 (1958).
8. B. R. Mottelson, Notes from Cours de l'École d'Été de Physique Théorique des Houches, 283 (1958).
9. A. Bohr and B. R. Mottelson (to be published).
10. S. T. Belyaev, Mat. Fys. Medd. Dan. Vid. Selsk. **31**, no. 11 (1959).
11. D. Bés, Nucl. Phys. **10**, 373 (1959).
21. D. R. Inglis, Phys. Rev. **96**, 1059 (1954); **97**, 901 (1955).
13. W. True and K. Ford, Phys. Rev. **109**, 1675 (1958).
14. A. M. Lane, Proceedings of the International Congress on Nuclear Physics, Paris (1958).
15. Numerous theoretical calculations for the single-particle levels have been made; for earlier references, see Ref. 5.
16. S. G. Nilsson, Mat. Fys. Medd. Dan. Vid. Selsk. **29**, no. 16 (1955).
17. L. A. Silverberg (to be published).
18. A. Bohr, Mottelson, and Pines, Phys. Rev. **110**, 936 (1958).
19. I. Bergström and G. Andersson, Arkiv Fysik **12**, 415 (1957).
20. Schmorak, Stockendal, McDonell, Bergström, and Gerholm, Nucl. Phys. **2**, 193 (1956–57).
21. We use the nuclear compilations of D. Strominger, J. M. Hollander, and G. T. Seaborg, Revs. Modern Phys. **30**, 585 (1958), and B. S. Dželepow and L. K. Peker, "Decay Schemes of Radioactive Nuclei" (Academy of Sciences of the USSR Press: Moscow, 1958).
22. P. H. Stelson and P. K. McGowan, Phys. Rev. **99**, 112 (1955).
23. F. K. McGowan and P. Stelson, Phys. Rev. **110**, 489 (1958).
24. Bayman, Reiner, and Sheline, Phys. Rev. **115**, 1627 (1959).
    K. W. Ford, Phys. Rev. **98**, 1516 (1955).
25. The mass data is taken from Nuclear Data Sheets, and from Everling, König, Mattauch, and Wapstra (to be published in Nucl. Phys.).
26. J. M. Blatt and V. F. Weisskopf, "Theoretical Nuclear Physics" (John Wiley and Sons: New York, 1952).
27. Demirkhanov, Gutin, and Dorokhov, JETP, U.S.S.R., **35**, 679 (1959).

28. H. HORIE and A. ARIMA, Phys. Rev. **99**, 778 (1955).
29. Conclusions similar to these have been drawn by K. W. FORD, Phys. Rev. **92**, 1094 (1953).
30. A. ARIMA and H. HORIE, Prog. Theor. Phys. (Japan) **12**, 623 (1954).
31. R. J. BLIN-STOYLE, Proc. Phys. Soc. A, 1158 (1953).
32. G. LAUKIEN, "Handbuch der Physik" XXXVIII/1 (Springer: Berlin, 1957), p. 120.
33. For the numerical calculations in the odd-A isotopes we have used the single-particle estimate from S. A. MOSZKOWSKI's article in Siegbahn, "Gamma and Beta Spectroscopy" (Interscience: New York, 1955). See the footnote on p. 69.
34. J. M. MIHELICH and R. D. HILL, Phys. Rev. **79**, 781 (1950).
35. M. E. ROSE, "Internal Conversion Coefficients" (North-Holland: Amsterdam, 1958).
36. ARIMA, HORIE, and SANO, Prog. Theor. Phys. (Japan) **17**, 567 (1957).
37. P. A. TOVE, Nuclear Instruments I, 95 (1957).
38. A. A. BARTLETT and G. REBKA, Bull. Am. Phys. Soc. ser. II, **3**, 64 (1958).
39. J. A. MCDONELL, R. STOCKENDALL, C. J. HERRLANDER, and I. BERGSTRÖM, Nucl. Phys. **3**, 513 (1957).
40. B. ASTROM, Arkiv Fysik **12**, 237 (1957).
41. See Cpt. III and Ref. 13.
42. ALDER, BOHR, HUUS, MOTTELSON, and WINTHER, Revs. Modern Phys. **28**, 432 (1956).
43. M. GOLDHABER and A. W. SUNYAR, Phys. Rev. **83**, 906 (1951).
44. ALKHAZEV, ANDREEV, ERELDINA, and LOMBERG, JETP, U.S.S.R., **33**, 1040 (1958).
45. P. H. STELSON and F. K. MCGOWAN, Bull. Am. Phys. Soc., Ser. II, **4**, 232 (1959).
46. S. OFER and A. SCHWARZSCHILD, Phys. Rev. Letters **3**, 384 (1959).